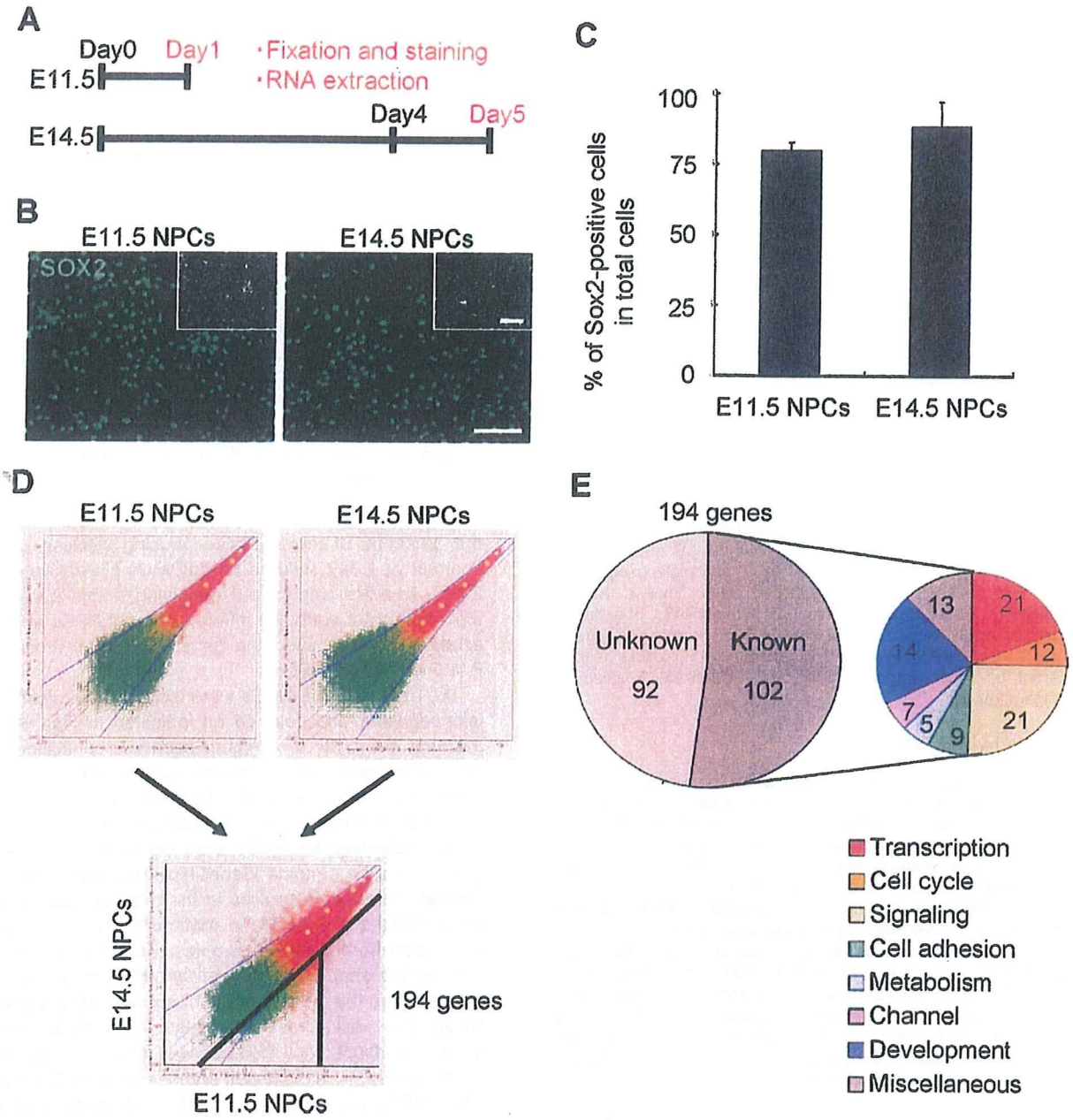

Fig. 1. Comparison of gene expression profiles in E11.5 and E14.5 NPCs. (A) Schematic of experimental protocol. NPCs isolated from E11.5 mouse telencephalon were plated (day 0) and used on the following day for immunostaining and RNA extraction (day 1). NPCs isolated at E14.5 were expanded for 4 days and replated on day 4. On day 5, these cells were fixed for immunostaining. RNA was also extracted. (B) E11.5 and E14.5 NPCs were stained with antibody against Sox2 (green). Scale bar=25 μm. Insets: Hoechst nuclear staining of each field. Scale bar=25 μm. (C) The percentage of Sox2-positive cells in E11.5 and E14.5 NPCs was quantified. Mean±S.D. (D) Scatter plots of E11.5 (upper left) and E14.5 (upper right) samples obtained from GeneChip analysis indicated no significant change between independent experiments with the same sample. Overview (lower plot) of gene expression change was compared between each sample. One hundred ninety-four genes were expressed at >fivefold higher level in E11.5 NPCs than E14.5 NPCs (light blue zone). (E) Of the 194 genes that were highly expressed in E11.5 NPCs, known genes were classified according to Affymetrix gene ontology. For interpretation of the references to color in this figure legend, the reader is referred to the Web version of this article.

Table 1. Transcription-related genes highly expressed in E11.5 NPCs

Probe set ID	GenBank ID	Gene symbol	E11.5 NPCs	E14.5 NPCs	E11.5/ E14.5
1433919_at	AV302111	*Asb4*	9.8	0.5	19.6
1419406_a_at	NM_016707	***Bcl11a***	13.8	1.8	7.7
1418271_at	NM_021560	***Bhlhb5***	10.6	1.2	8.8
1452207_at	Y15163	*Cited2*	16.7	2.6	6.4
1449470_at	NM_010053	*Dlx1*	13.8	2.4	5.8
1448877_at	NM_010054	*Dlx2*	9.8	1.8	5.4
1449863_a_at	NM_010056	*Dlx5*	11.2	0.7	16.0
1459211_at	AW546128	*Gli2*	8.0	1.5	5.3
1456067_at	AW546010	*Gli3*	20.6	2.1	9.8
1422851_at	X58380	***Hmga2***	25.5	0.5	51.0
1450723_at	BQ176915	*Ils1*	8.6	0.1	86.0
1427300_at	D49658	*Lhx8*	10.5	0.1	105.0
1417155_at	BC005453	***N-myc***	8.2	1.2	6.8
1415811_at	BB702754	*NP95*	12.6	2.1	6.0
1421193_a_at	NM_016768	*Pbx3*	12.3	1.6	7.7
1417400_at	NM_030690	*Rai14*	11.0	1.6	6.9
1435856_x_at	AV310148	*Smarcb1*	8.0	1.6	5.0
1431255_at	BB656631	***Sox11***	38.7	6.2	6.2
1450034_at	AW214029	*Stat1*	9.6	1.8	5.3
1416711_at	NM_009322	*Tbr1*	9.8	0.2	49.0
1423424_at	BB732077	*Zic3*	11.2	0.5	22.4

Genes reported to participate in cell growth, differentiation and chromatin remodeling are shown in boldface.

Spatio-temporal expression patterns of genes highly expressed in E11.5 NPCs

To substantiate the GeneChip results, we extracted RNA from E11.5 and E14.5 NPCs and performed real-time RT-PCR using specific primers for each selected gene. Consistent with the GeneChip analysis, all five genes were highly expressed in E11.5 NPCs compared with E14.5 NPCs (Fig. 2A). We next performed *in situ* hybridization for each gene using E11.5, E14.5 and E17.5 mouse brain sections (Fig. 2B). *N-myc* and *Hmga2* mRNAs were specifically detected in the ventricular zone (VZ) of E11.5 brain, implying that N-myc and Hmga2 play some role in NPCs at this stage. By contrast, *Bhlhb5*, *Sox11* and *Bcl11a* expression was stronger in cortical plate, where postmitotic neurons reside, than in the VZ (Fig. 2B). We therefore decided to analyze the function of N-myc and Hmga2 in more detail.

Transduction of *N-myc* and *Hmga2* inhibits astrocyte differentiation of E14.5 NPCs

We next examined whether N-myc and Hmga2 affect astrocyte differentiation of NPCs. We expressed EGFP alone (control), and EGFP together with either N-myc or Hmga2, using retroviral infection in E14.5 NPCs, in which expression of the endogenous genes is very low. Virus-infected E14.5 NPCs were cultured for 4 days in the presence of LIF to induce astrocyte differentiation, and then stained with antibodies against GFP and GFAP. As shown in Fig. 3A and B, NPCs infected with control virus effectively differentiated into GFAP-positive astrocytes in response to LIF stimulation (42±2.6%). In contrast, GFAP-positive astrocyte differentiation was virtually abolished in cells ectopically expressing N-myc (0.5±0.4%) and Hmga2 (3±2.0%) (Fig. 3A, B). Expression of these genes did not significantly affect neuronal differentiation of NPCs, as assessed by monitoring expression of the neuronal marker βIII-tubulin, compared with the control cells (Fig. 3C, D). We further examined whether the observed suppression of astrocyte differentiation of NPCs infected with viruses encoding N-myc or Hmga2 could be attributed to specific cell-growth inhibition or to cell death. To address this issue, we performed immune staining for the cycling cell marker Ki67 and the apoptotic marker cleaved caspase 3. Although proliferation of NPCs ectopically expressing N-myc or Hmga2 appeared to be slightly enhanced, expression of either gene caused negligible cell death. These results suggest that N-myc and Hmga2 inhibit astrocyte differentiation of NPCs by a mechanism distinct from that of the neurogenic bHLH factors, which enhance neuronal differentiation (Sun et al., 2001).

Continuous expression of N-myc and Hmga2 in E11.5 NPCs fails to preserve the hypermethylated status of an astrocyte-specific gene promoter

We have previously shown that the *gfap* promoter is highly methylated in E11.5 NPCs, and becomes demethylated as gestation proceeds (Takizawa et al., 2001). This demethylation enables NPCs at later developmental stages, E14.5 or thereafter, to respond to LIF and differentiate into GFAP-positive astrocytes. As shown in the foregoing data, expression levels of *N-myc* and *Hmga2* thus seemed to be reduced concurrently with the developmental stage-dependent demethylation of an astrocyte-specific gene promoter; furthermore, ectopic expression of these genes in E14.5 NPCs inhibited GFAP-positive astrocyte differentiation. We therefore hypothesized that sustained expression of N-myc and Hmga2 in E11.5 NPCs might maintain the hypermethylated status of the *gfap* promoter. To test this, we infected E11.5 NPCs with viruses expressing EGFP alone and EGFP together with either N-myc or Hmga2 and cultured them for 4 days. GFP-positive cells were sorted by FACS and their genomic DNAs were extracted for bisulfite sequencing. As observed in the previous study (Takizawa et al., 2001), the *gfap* promoter including the STAT3 site became demethylated to about 65% in control virus-infected cells after the 4-day culture, and this was also the case for both N-myc- and Hmga2-expressing virus-infected cells (Fig. 3E, F). These results indicate that sustained expression of N-myc and Hmga2 in E11.5 NPCs does not affect the process of demethylation in this astrocyte-specific gene promoter. On the other hand, when 4-day-cultured control virus-infected E11.5 NPCs were then stimulated with LIF for an additional 4 days, GFAP-positive astrocytes appeared, probably due to demethylation in the promoter, whereas neither *N-myc* nor *Hmga2* virus-infected cells gave rise to astrocytes even in the presence of LIF (data not shown). These results suggest that N-myc and Hmga2 inhibit precocious astrocyte differentiation of midgestational NPCs independent of the DNA methylation status of an astrocyte-specific gene promoter.

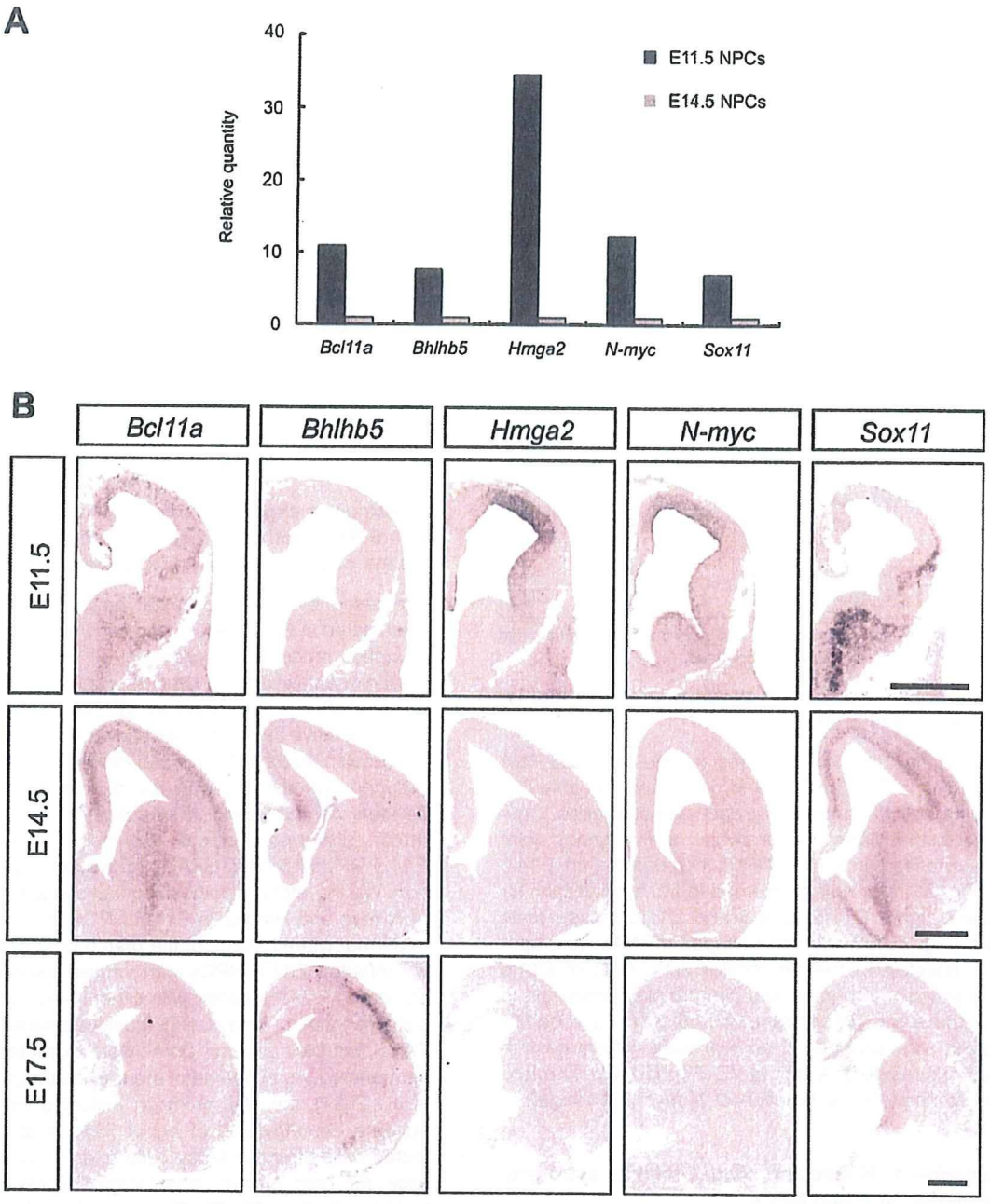

Fig. 2. *N-myc* and *Hmga2* are highly expressed in the VZ of E11.5 mouse brain. (A) Gene-specific real-time RT-PCR was performed to validate GeneChip analysis data. (B) *In situ* hybridization was performed for E11.5, E14.5 and E17.5 mouse brain sections. No signal was detected when sense-probes for each gene were used (data not shown). Scale bar=500 μm.

DISCUSSION

In this study, we compared NPC gene expression profiles at different developmental stages using Affymetrix GeneChips and the Percellome method, and then analyzed by *in situ* hybridization the spatio-temporal expression patterns of genes which were highly expressed in E11.5 NPCs. We found that *N-myc* and *Hmga2* were specifically expressed in E11.5 NPC both *in vivo* and *in vitro* and, furthermore, that the transduction of these genes into NPCs suppressed LIF-induced astrocytic differentiation without affecting DNA demethylation of the astrocyte-specific *gfap* gene promoter.

The basic HLH leucine zipper transcription factor N-myc,a member of the myc family of oncogenes, is a nuclear phosphoprotein exhibiting site-specific DNA-binding activity (Ramsay et al., 1986; Alex et al., 1992), and has

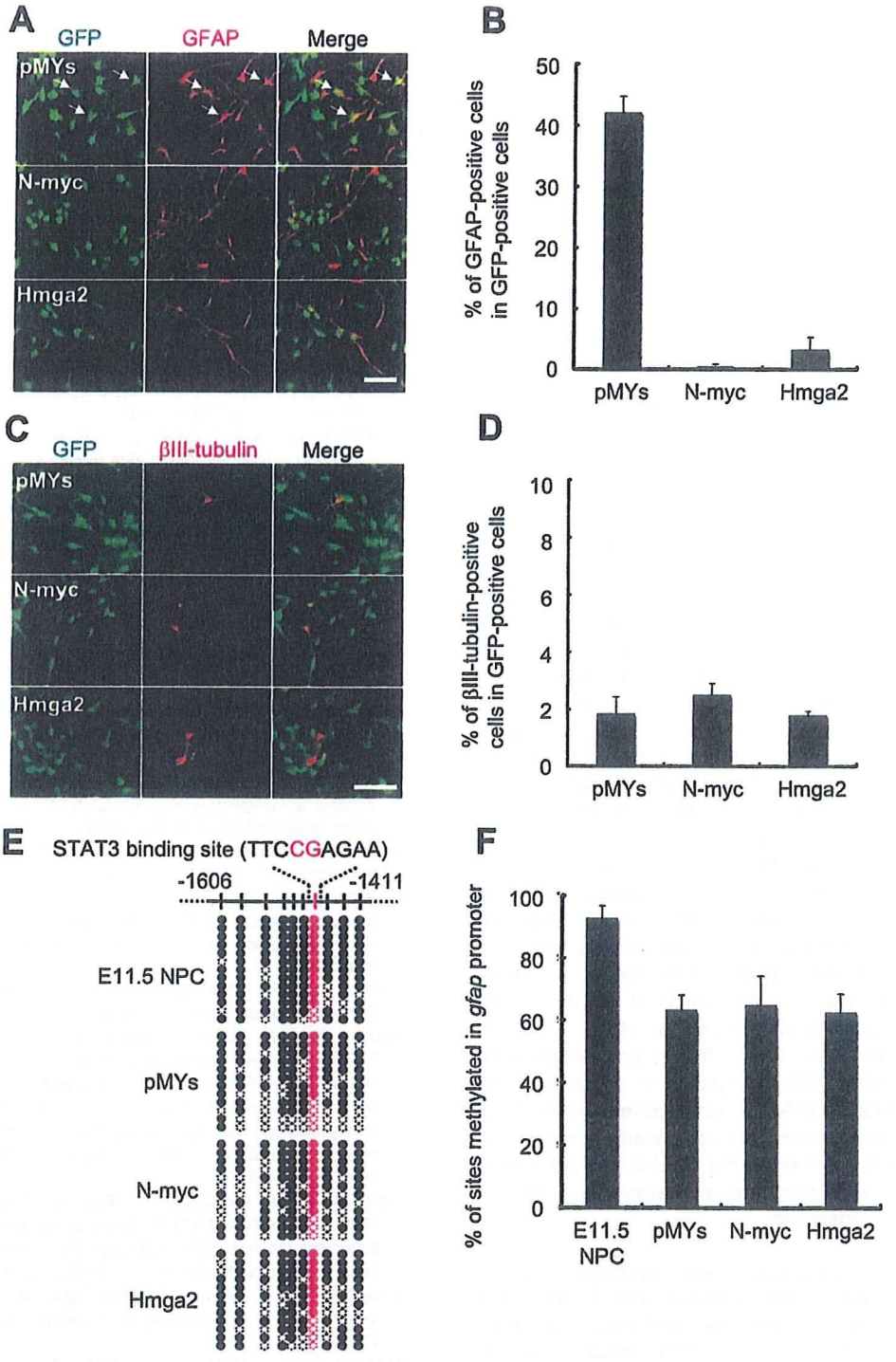

Fig. 3. N-myc and Hmga2 inhibit astrocyte differentiation of NPCs even in the presence of LIF. (A–D) E14.5 NPCs were infected with recombinant retroviruses engineered to express *EGFP* alone (pMYs), and *EGFP* together with either *N-myc* (N-myc) or *Hmga2* (Hmga2), and cultured with LIF (50 ng/ml) for 4 days to induce astrocyte differentiation. The cells were then stained with antibodies against GFP (green) and GFAP (red) (A). Arrows indicate GFP/GFAP double-positive cells. The percentage of GFAP-positive astrocytes in GFP-positive cells was quantified (B). Mean±S.D. The cells were also stained with antibodies against GFP (green) and βIII-tubulin (red) (C). The percentage of βIII-tubulin-positive neurons in GFP-positive cells was quantified (D). Mean±S.D. (E) E11.5 NPCs were infected with recombinant retroviruses engineered to express *EGFP* alone (pMYs), and *EGFP* together with either *N-myc* (N-myc) or *Hmga2* (Hmga2), and subsequently cultured for 4 days. GFP-positive cells were then sorted based on GFP fluorescence, and genomic DNA was extracted for bisulfite sequencing. White and black circles indicate unmethylated and methylated CpG sites, respectively. The E11.5 NPC sample was freshly prepared NPCs from telencephalon at E11.5. The CpG dinucleotide within the STAT3 binding site is indicated in red. (F) Methylation frequency in the *gfap* promoter. Mean±S.D. Scale bars=50 μm (A, C). For interpretation of the references to color in this figure legend, the reader is referred to the Web version of this article.

been reported to be expressed in a wide range of vertebrate tissues, primarily during embryogenesis (Schreiber-Agus et al., 1993). The mice deficient for functional *N-myc* are embryonic lethal (Stanton et al., 1992). Since N-myc has been shown to be a transcriptional activator, it may inhibit astrocyte differentiation via induction of neurogenic bHLH factors such as *Ngn1* (Sun et al., 2001), which have already been suggested to inhibit astrocyte differentiation in midgestational NPCs. However, this scenario seems unlikely because *N-myc* expression in NPCs did not affect neuronal differentiation, as assessed by monitoring expression of the neuronal marker βIII-tubulin (Fig. 3C, D). On the other hand, Hmga2 possesses an acidic C-terminal tail and three individual DNA-binding domains which bind short stretches of AT-rich DNA with high affinity (Reeves, 2001). *Hmga2* is expressed in pluripotent embryonic stem (ES) cells and in most tissues and organs during embryogenesis, but at very low levels or not at all in adult tissues (Zhou et al., 1995). Its function appears to be critical for cell growth, because mice lacking functional *Hmga2* exhibit a pygmy phenotype (Zhou et al., 1995). Recently, it was reported that Hmga2 specifically accumulates on senescent cell chromatin and that it functions as a structural component of senescence-associated heterochromatin foci and as a repressor of proliferation-associated genes (Narita et al., 2006). We therefore expected that Hmga2 would maintain the hypermethylation status of the astrocyte-specific *gfap* promoter via transcription-repressive heterochromatin formation in E11.5 NPCs. However, our results indicate that this is not the case. The mechanism(s) whereby N-myc and Hmga2 inhibit astrocyte differentiation must await further investigation.

Although DNA methylation is a critical cell-intrinsic determinant for the neurogenic-to-astrogliogenic switch and/or astrocyte differentiation of NPCs, many other spatio-temporally expressed extracellular factors such as CT-1, Notch and Wnt1 (Barnabe-Heider et al., 2005; Hirabayashi and Gotoh, 2005; Nagao et al., 2007) and intracellular factors including Ngn (Sun et al., 2001), N-CoR (Hermanson et al., 2002), N-myc and Hmga2 (this study) complement DNA methylation to ensure the sequential differentiation of NPCs during development. Thus, to better understand the mechanism underlying these processes, this study emphasizes the need to take cell-extrinsic cues, cell-intrinsic programs and factors, and their interaction into consideration.

Acknowledgments—We thank Dr. T. Kitamura (Tokyo University) for pMY vector and Plat-E cells. We appreciate Dr. Y. Bessho and T. Matsui for valuable discussions. We also thank Dr. I. Smith for helpful comments and critical reading of the manuscript. We are very grateful to N. Ueda for excellent secretarial assistance. Many thanks to N. Namihira for technical help. We also thank N. Moriyama for technical help with GeneChip analysis. This work has been supported by a Grant-in-Aid for Science Research on Priority Areas and the NAIST Global COE Program (Frontier Biosciences: Strategies for survival and adaptation in a changing global environment) from the Ministry of Education, Culture, Sports, Science and Technology (MEXT) of Japan.

REFERENCES

Abramova N, Charniga C, Goderie SK, Temple S (2005) Stage-specific changes in gene expression in acutely isolated mouse CNS progenitor cells. Dev Biol 283:269–281.

Ajioka I, Maeda T, Nakajima K (2006) Identification of ventricular-side-enriched molecules regulated in a stage-dependent manner during cerebral cortical development. Eur J Neurosci 23:296–308.

Alex R, Sozeri O, Meyer S, Dildrop R (1992) Determination of the DNA sequence recognized by the bHLH-zip domain of the N-Myc protein. Nucleic Acids Res 20:2257–2263.

Barnabe-Heider F, Wasylnka JA, Fernandes KJ, Porsche C, Sendtner M, Kaplan DR, Miller FD (2005) Evidence that embryonic neurons regulate the onset of cortical gliogenesis via cardiotrophin-1. Neuron 48:253–265.

Bonni A, Sun Y, Nadal-Vicens M, Bhatt A, Frank DA, Rozovsky I, Stahl N, Yancopoulos GD, Greenberg ME (1997) Regulation of gliogenesis in the central nervous system by the JAK-STAT signaling pathway. Science 278:477–483.

Brunelli S, Innocenzi A, Cossu G (2003) Bhlhb5 is expressed in the CNS and sensory organs during mouse embryonic development. Gene Expr Patterns 3:755–759.

Bugga L, Gadient RA, Kwan K, Stewart CL, Patterson PH (1998) Analysis of neuronal and glial phenotypes in brains of mice deficient in leukemia inhibitory factor. J Neurobiol 36:509–524.

Cai L, Morrow EM, Cepko CL (2000) Misexpression of basic helix-loop-helix genes in the murine cerebral cortex affects cell fate choices and neuronal survival. Development 127:3021–3030.

Edlund T, Jessell TM (1999) Progression from extrinsic to intrinsic signaling in cell fate specification: a view from the nervous system. Cell 96:211–224.

Graham V, Khudyakov J, Ellis P, Pevny L (2003) SOX2 functions to maintain neural progenitor identity. Neuron 39:749–765.

He F, Ge W, Martinowich K, Becker-Catania S, Coskun V, Zhu W, Wu H, Castro D, Guillemot F, Fan G, de Vellis J, Sun YE (2005) A positive autoregulatory loop of Jak-STAT signaling controls the onset of astrogliogenesis. Nat Neurosci 8:616–625.

Hermanson O, Jepsen K, Rosenfeld MG (2002) N-CoR controls differentiation of neural stem cells into astrocytes. Nature 419: 934–939.

Hirabayashi Y, Gotoh Y (2005) Stage-dependent fate determination of neural precursor cells in mouse forebrain. Neurosci Res 51: 331–336.

Hsieh J, Gage FH (2004) Epigenetic control of neural stem cell fate. Curr Opin Genet Dev 14:461–469.

Kanno J, Aisaki K, Igarashi K, Nakatsu N, Ono A, Kodama Y, Nagao T (2006) "Per cell" normalization method for mRNA measurement by quantitative PCR and microarrays. BMC Genomics 7:64.

Knoepfler PS, Cheng PF, Eisenman RN (2002) N-myc is essential during neurogenesis for the rapid expansion of progenitor cell populations and the inhibition of neuronal differentiation. Genes Dev 16:2699–2712.

Koblar SA, Turnley AM, Classon BJ, Reid KL, Ware CB, Cheema SS, Murphy M, Bartlett PF (1998) Neural precursor differentiation into astrocytes requires signaling through the leukemia inhibitory factor receptor. Proc Natl Acad Sci U S A 95:3178–3181.

Morita S, Kojima T, Kitamura T (2000) Plat-E: an efficient and stable system for transient packaging of retroviruses. Gene Ther 7: 1063–1066.

Nagao M, Sugimori M, Nakafuku M (2007) Cross talk between notch and growth factor/cytokine signaling pathways in neural stem cells. Mol Cell Biol 27:3982–3994.

Nakashima K, Wiese S, Yanagisawa M, Arakawa H, Kimura N, Hisatsune T, Yoshida K, Kishimoto T, Sendtner M, Taga T (1999a) Developmental requirement of gp130 signaling in neuronal survival and astrocyte differentiation. J Neurosci 19:5429–5434.

Nakashima K, Yanagisawa M, Arakawa H, Kimura N, Hisatsune T, Kawabata M, Miyazono K, Taga T (1999b) Synergistic signaling in

fetal brain by STAT3-Smad1 complex bridged by p300. Science 284:479–482.

Narita M, Krizhanovsky V, Nunez S, Chicas A, Hearn SA, Myers MP, Lowe SW (2006) A novel role for high-mobility group a proteins in cellular senescence and heterochromatin formation. Cell 126: 503–514.

Nieto M, Schuurmans C, Britz O, Guillemot F (2001) Neural bHLH genes control the neuronal versus glial fate decision in cortical progenitors. Neuron 29:401–413.

Rajan P, McKay RD (1998) Multiple routes to astrocytic differentiation in the CNS. J Neurosci 18:3620–3629.

Ramsay G, Stanton L, Schwab M, Bishop JM (1986) Human proto-oncogene N-myc encodes nuclear proteins that bind DNA. Mol Cell Biol 6:4450–4457.

Reeves R (2001) Molecular biology of HMGA proteins: hubs of nuclear function. Gene 277:63–81.

Saiki Y, Yamazaki Y, Yoshida M, Katoh O, Nakamura T (2000) Human EVI9, a homologue of the mouse myeloid leukemia gene, is expressed in the hematopoietic progenitors and down-regulated during myeloid differentiation of HL60 cells. Genomics 70:387–391.

Sawai S, Kato K, Wakamatsu Y, Kondoh H (1990) Organization and expression of the chicken N-myc gene. Mol Cell Biol 10:2017–2026.

Schreiber-Agus N, Horner J, Torres R, Chiu FC, DePinho RA (1993) Zebra fish myc family and max genes: differential expression and oncogenic activity throughout vertebrate evolution. Mol Cell Biol 13:2765–2775.

Sock E, Rettig SD, Enderich J, Bosl MR, Tamm ER, Wegner M (2004) Gene targeting reveals a widespread role for the high-mobility-group transcription factor Sox11 in tissue remodeling. Mol Cell Biol 24:6635–6644.

Stanton BR, Perkins AS, Tessarollo L, Sassoon DA, Parada LF (1992) Loss of N-myc function results in embryonic lethality and failure of the epithelial component of the embryo to develop. Genes Dev 6:2235–2247.

Sun Y, Nadal-Vicens M, Misono S, Lin MZ, Zubiaga A, Hua X, Fan G, Greenberg ME (2001) Neurogenin promotes neurogenesis and inhibits glial differentiation by independent mechanisms. Cell 104:365–376.

Takizawa T, Nakashima K, Namihira M, Ochiai W, Uemura A, Yanagisawa M, Fujita N, Nakao M, Taga T (2001) DNA methylation is a critical cell-intrinsic determinant of astrocyte differentiation in the fetal brain. Dev Cell 1:749–758.

Temple S (2001) The development of neural stem cells. Nature 414:112–117.

Tomita K, Moriyoshi K, Nakanishi S, Guillemot F, Kageyama R (2000) Mammalian achaete-scute and atonal homologs regulate neuronal versus glial fate determination in the central nervous system. EMBO J 19:5460–5472.

Zhou X, Benson KF, Ashar HR, Chada K (1995) Mutation responsible for the mouse pygmy phenotype in the developmentally regulated factor HMGI-C. Nature 376:771–774.

(Accepted 13 June 2008)
(Available online 21 June 2008)

Available online at www.sciencedirect.com
ScienceDirect
Biochemical and Biophysical Research Communications 365 (2008) 562–567
BBRC
www.elsevier.com/locate/ybbrc

Inducibility of cytochrome P450 1A1 and chemical carcinogenesis by benzo[*a*]pyrene in AhR repressor-deficient mice

Tomonori Hosoya [a,c,1], Nobuhiko Harada [a,b,1], Junsei Mimura [a,d], Hozumi Motohashi [a,b], Satoru Takahashi [b], Osamu Nakajima [a], Masanobu Morita [a], Shimako Kawauchi [a], Masayuki Yamamoto [a,b,c], Yoshiaki Fujii-Kuriyama [a,d,*]

[a] *Center for Tsukuba Advanced Research Alliance, University of Tsukuba, 1-1-1 Tennodai, Tsukuba 305-8577, Japan*
[b] *Graduate School of Comprehensive Human Science, University of Tsukuba, 1-1-1 Tennodai, Tsukuba 305-8577, Japan*
[c] *Exploratory Research for Advanced Technology, Japan Science and Technology Agency, 4-1-8 Honcho, Kawaguchi, Saitama 332-0012, Japan*
[d] *Solution Oriented Research for Science and Technology, Japan Science and Technology Agency, 4-1-8 Honcho, Kawaguchi, Saitama 332-0012, Japan*

Received 30 October 2007
Available online 20 November 2007

Abstract

AhR repressor (AhRR) is an AhR-related bHLH-PAS transcription factor. It is known to repress AhR transcription activity in a competitive manner. To examine AhRR functions in mice, we produced AhRR-deficient mice by gene knockout. *AhRR(−/−)* mice were born in normal Mendelian proportions, grew well, and were fertile. *AhR(−/−)* mice exhibited higher levels of *Cyp1a1* (Cytochrome P450 1A1) mRNA induction in the skin, stomach and spleen than wild-type mice, while expression of *Cyp1a1* mRNA was not significantly altered in the liver, lung, heart or other tissues, suggesting that "super-induction" of *Cyp1a1* mRNA expression in *AhRR(−/−)* mice occurs in a tissue specific manner. *AhRR(−/−)* mice displayed a delayed response to skin carcinogenesis caused by benzo[*a*]pyrene. Since CYP1A1 is involved in the metabolic activation and detoxification of chemical carcinogens, these results suggest that overexpression of CYP1A1 shifts the balance of the metabolic activities in the skin of *AhRR(−/−)* mice in favor of the detoxification of carcinogens.
© 2007 Elsevier Inc. All rights reserved.

Keywords: AhR receptor; Gene targeting; Chemical carcinogenesis; CYP1A1; AhR; Transcription; Metabolic activation; Polyaromatic hydrocarbon; Super-induction; Transcription repression

Aryl hydrocarbon receptor (AhR) is a ligand-activated transcription factor belonging to the bHLH (basic helix-loop-helix)-PAS (Per-Arnt-Sim homology) superfamily [1–3]. Normally, AhR exists in the cytoplasm in association with the HSP90 complex. Upon binding with its ligands, such as 3MC (3-methylcholanthrene) and TCDD (2′,3′,7′,8′-tetrachlorodibenzo-*p*-dioxin), AhR translocates to the nucleus, where it heterodimerizes with Arnt (AhR nuclear translocator, another member of the bHLH-PAS superfamily) to induce the expression of a battery of drug-metabolizing enzymes including CYP1A1, 1B1 and 1A2 [1–3]. In addition, recently, the target genes of AhR have been expanded to those involved in cell cycle regulation, apoptosis, endocrine regulation and the immune system [4,5]. Among them, AhRR is unique, because it represses the transcriptional activity of AhR and thus forms a negative feedback regulatory loop in the xenobiotic signal tranduction pathway [6,7]. AhRR (AhR repressor) which was originally identified in mice, has also been reported in many animal species including human [8], rat [9] and fish [10]. In cell culture, AhRR inhibits AhR transcription activity by competing with AhR for heterodimer formation with Arnt; the AhRR/Arnt heterodimer then competes with AhR/Arnt heterodimer for binding to xeno-

* Corresponding author. Address: Center for Tsukuba Advanced Research Alliance, University of Tsukuba, 1-1-1 Tennodai, Tsukuba 305-8577, Japan. Fax: +81 29 853 7318.
E-mail address: ykfujii@tara.tsukuba.ac.jp (Y. Fujii-Kuriyama).
[1] These authors contributed equally to this work.

0006-291X/$ - see front matter © 2007 Elsevier Inc. All rights reserved.
doi:10.1016/j.bbrc.2007.11.016

biotic response element (XRE) sequences [6]. Little is known, however, about the functional role of AhRR in the AhR signaling pathway in living animals.

To investigate the functional roles of AhRR in the AhR signaling system *in vivo*, we generated *AhRR(−/−)* mice by homologous recombination. *AhRR(−/−)* mice were born in normal Mendelian propotions, grew well, and were fertile. We found that *AhRR(−/−)* mice were relatively resistant to skin carcinogenesis induced by benzo[*a*]pyrene (B[*a*]P), compared with the wild type (WT). Skin fibroblast cells derived from *AhRR(−/−)* mice showed a remarkably higher level of *Cyp1a1* mRNA induction in response to B[*a*]P than WT counterparts. This "super-induction" of *Cyp1a1* mRNA was not observed in all the tissues examined of *AhRR(−/−)* mice, indicating that AhRR works as repressor of AhR only in specific tissues.

Materials and methods

Generation of AhRR-deficient mice. We disrupted the AhRR gene in mouse embryonic stem cells as described [11]. A targeting vector was constructed by replacing a part of the 2nd exon and the 2nd intron of the *AhRR* gene with the *NLS-LacZ-neo*^{r} gene cassette as shown in Fig. 1A. The HSV-TK gene was used for negative selection. The linearized targeting vector was electroporated into E14 ES cells, and the cells were subjected to double selection with G418 (0.3 mg/ml) and gancyclovir (2 μM). Double-resistant ES clones were then screened by PCR using a pair of oligonucleotide primers corresponding to the neomycin resistance gene (TV-neo; 5′-TCA GAG CAG CCG ATT GTC TGT TGT GCC CAG TCA T-3′) and *AhRR* gene (AhRR TV-PCR2-2; 5′-AGA CCT GAG AGG TCT AGA CTT GGA TGC TAC-3′) depicted in Fig. 1A as arrowheads. To confirm the homologous recombination, ES clone genomic DNA was digested with PstI or BamHI restriction enzymes for DNA blot analysis using 5′ or 3′ external probes. Positive ES clones were injected into blastocoel cavities of 3.5-day postcoitum (dpc) blastocysts derived from C57BL/6 mice. The injected blastocysts were surgically transplanted into the uteri of pseudo-pregnant ICR recipient mice at 2.5 dpc. Germ-line transmission of the *AhRR* defective allele was screened by PCR to obtain two independently targeted founder mice, and heterozygous F1 mice were intercrossed to obtain *AhRR(−/−)* mice. Tail DNAs of the pups were extracted and subjected to PCR for the presence of the mutated *AhRR* allele using the TV-neo and AhRR TV-PCR2-2 primers. To distinguish easily the mutated *AhRR* alleles from WT by PCR, the following oligonucleotides were used as PCR primers: AhRR KO-5′ (5′-GAA ACT GTA GCC CTG GAT ACT TCT G-3′), AhRR KO-3′ (5′-ATC ATT GCT CTG AGC ATC CAC TAG G-3′) and TV neo primer. The AhRR KO-5′ and 3′ primer pair amplifies only the *AhRR* wild-type allele (190 bp), while that of the AhRR KO-3′ and TV neo primers amplifies only the mutated one (527 bp).

PCR-RFLP analysis. Because the established *AhRR* mutant mice contain both C57BL/6 and 129Sv *AhR* alleles, PCR-restriction fragment length polymorphism (RFLP) analysis was performed to exclude the 129Sv *AhR* allele, as described [8,12]. Briefly, tail genomic DNAs were amplified by PCR with a primers OL72 (5′-GGT TCG AAT TTC CAG GAT GG-3′) and OL111 (5′-CCA CCC CAG GTA CAT GAT GGA ACC-3′). PCR fragments were digested with *Eco47*III restriction enzyme and electrophoresed on an 8.0% acrylamide gel. The C57BL/6 *AhR* allele yields 142 and 76 bp fragments, while the 129Sv *AhR* allele yields a 218 bp fragment. Mice homozygous for the C57BL/6 *AhR* allele were used for further analyses.

Chemical treatment and tumor induction. B[*a*]P and 3MC were obtained from Wako Junyaku Co. (Osaka). To analyze *Cyp1a1* induction in mouse tissues, corn oil (vehicle control) or 3MC dissolved in corn oil (4 mg/ml) was intraperitoneally injected into mice (80 mg/kg body weight), and the mice were sacrificed 24 or 48 h after injection. Tissues were collected from the mice and subjected to RNA extraction for RT-PCR analysis, as described [6]. For tumor induction experiments, *AhRR(−/−)* mice were backcrossed with wild-type C57BL/6 mice for at least 7 generations, and subcutaneously injected with 0.2 ml of B[*a*]P in corn oil (10 mg/ml) twice, a week apart, as described [13]. All mice of 8 weeks of age were examined for development of tumors at least once a week for 30 weeks until death. The tumor sizes were recorded throughout the experimental period. Tumor-bearing mice were counted and presented as percentage of the total. Tumors were dissected, fixed in formalin and embedded in paraffin. Sections at 3-μm thickness were stained with hematoxylin and eosin as described previously [14].

Skin fibroblast cell culture preparation. WT and *AhRR(−/−)* skin fibroblast cultures were prepared from the skin of at least six neonatal mice, respectively. Skin was removed from newborn mice, and then minced into small pieces, followed by digestion with 1% collagenase (SIGMA) in DMEM for 1 h at 37 °C. The digests were then rinsed once with PBS, then maintained in DMEM supplemented with 10% FBS and penicillin/streptomycin at 37 °C in 5% CO_2 until skin fibroblast cells covered the entire culture dish plate. The cells were replated at 2.0×10^6 cells per 10 cm diameter dish for further experiments and passage.

Cell treatments and RT-PCR. Skin fibroblast cell cultures were incubated in the absence (DMSO) or presence of 1 μM B[*a*]P (DMSO solution) as described in figure legends. Total RNA was extracted from the cells with TRIsure RNA extraction reagent and reverse-transcribed into cDNA by using SuperScript II RTase. Quantitative gene expression analysis was

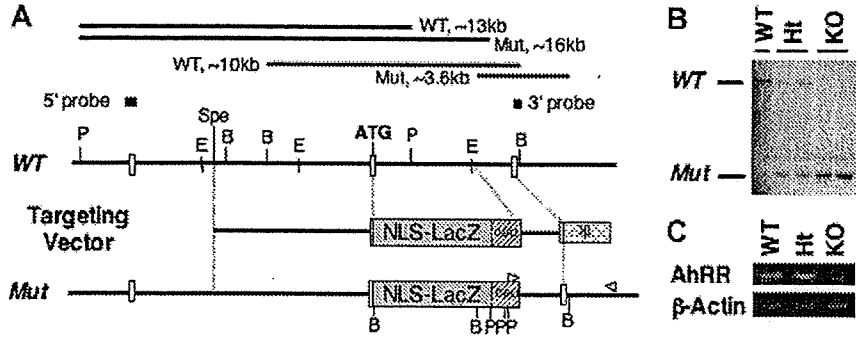

Fig. 1. Targeted disruption of the mouse *AhRR* gene. (A) Schematic representation of the targeting vector, *AhRR*-WT and Mut alleles. Cleavage sites for the restriction enzymes are indicated by E (EcoRI), B (BamHI), Sp (SpeI) and P (PstI). The locations of the 5′ and 3′ probes used for the DNA blot analysis are indicated at the top. Two arrowheads indicate the position of primers used to identify homologous recombinant clones. (B) DNA blot of mouse genome using the 3′ probe. Genomic DNA (10 μg) was digested with BamHI; digested products were then electrophoresed and hybridized. (C) Mice were treated with 3MC for 24 h, and then total RNA from spleen was subjected to RT-PCR analysis.

performed by using Platinum SYBRGreen qPCR premix in an ABI7300 qPCR analyzer. PCR primers for CYP1A1: 5′-GGACATTTGAGAA GGGCCAC-3′ and 5′-CGTCCAGCTTCCTGTCCTGA-3′; for CYP1B1: 5′-GGATGTGCCTGCCACTATTAC-3′, 5′-CCTGAACATCCGGGTA TCTG-3′; for AhRR; 5′-CCTGTCCCGGGATCAAAGATG-3′ and 5′-CTCACCACCAGAGCGAAGCCATTGA-3′; for β-actin: 5′-GTGAAA AGATGACCCAGATCATG-3′ and 5′-GTGGTACGACCAGAGGCA TAC-3′.

β-Galactosidase staining. Tissues were fixed overnight in PBS containing 4% paraformaldehyde, dehydrated with ethanol, embedded in paraffin and sectioned at 3-μm thickness. The sections were dewaxed and stained. β-galactosidase staining was carried out as described [15].

Results

Targeted disruption of mouse AhRR gene

To investigate the functional role of AhRR *in vivo*, we generated an *AhRR* knockout mouse by gene targeting technology as described [15]. The *NLS-LacZ* sequence was fused in a reading frame with the 8th amino acid of the *AhRR* gene so that the inserted *NLS-LacZ* gene could mimic the mode of *AhRR* gene expression (Fig. 1A). Since the resulting protein product lacks most of the coding region of the bHLH domain, which is essential for dimerization and DNA binding, we expected that the knockout mice would lack AhRR function. E14 embryonic stem (ES) cells were electroporated with the linearized targeting vector and subjected to positive-negative selection. Of the 360 clones screened by PCR, nine clones had undergone homologous recombination at the *AhRR* locus, as subsequently confirmed by DNA blot (Fig. 1B). The mutant clones were proliferated and microinjected into C57BL/6 recipient blastocysts to generate chimeric mice, and the male chimeras were crossed with C57BL/6 females. Ultimately, two independent mutant ES cells were successfully transmitted to offspring.

Generation of homozygous AhRR mutant mice

AhRR(+/−) mutant mice were viable and fertile, and were intercrossed for analysis of the phenotypes of *AhRR(−/−)* homozygosity. Offspring of all three genotypes were born at a normal Mendelian proportion in both mixed and C57BL/6 backgrounds (Table 1).

To assess complete inactivation of the gene, the absence of *AhRR* mRNA was confirmed by RT-PCR. Intraperitoneal injection of 3MC induced *AhRR* mRNA expression in the heart of wild-type and *AhRR(+/−)* mice, whereas *AhRR* mRNA was not found in the *AhRR(−/−)* (Fig. 1C). Taken together with the results of the DNA blots (Fig. 1B), these results confirmed the specific disruption of the *AhRR* gene.

Table 1
Genotypes of offspring obtained by double heterozygous mating

Background[a]	WT	Ht	KO	*n*
Mix	63 (20.3%)	166 (53.4%)	82 (26.4%)	311
B6	30 (30.6%)	49 (50.0%)	19 (19.4%)	98

[a] Mating was performed with heterozygous mice in C57BL/6 and 129SV background (Mix) or mice backcrossed to C57BL/6 background 7 generations (B6).

The general behaviors including feeding, growth and mating of AhRR*(−/−)* mice were apparently normal, and the mutants lived a normal lifespan (data not shown). Gross anatomy did not reveal any anomaly in AhR*(−/−)* mice.

Gene expression in AhRR(−/−) mice

To investigate the repressor function of AhRR *in vivo*, 3MC was intraperitoneally injected into *AhRR(−/−)* and WT mice. After 24 h of treatment, expression levels of *Cyp1a1* mRNA, one of the well-known AhR target gene products, were measured in various tissues along with the levels of *AhRR* mRNA (Fig. 2A). As previously observed [6], in WT mice, *AhRR* mRNA was highly induced by 3MC in heart, lung, and spleen, and weakly in liver, kidney, thymus intestine, brain and stomach. On the other hand, *Cyp1a1* mRNA was highly induced in lung, liver and heart in WT mice, while this high induction was not much affected in the same tissues of *AhRR(−/−)* mice. In spleen and stomach, induction level of *Cyp1a1* mRNA was higher in *AhRR(−/−)* mice than in WT. The higher induction of *Cyp1a1* mRNA in *AhRR(−/−)* than in WT mice was not observed in all the tissues examined, i.e., induction was tissue-dependent.

We performed a time-course study of *Cyp1a1* mRNA expression in the 3MC-injected mouse spleen (Fig. 2B). In WT mice, *Cyp1a1* mRNA was gradually increased and reached a plateau at 48 h after the 3MC injection. In contrast, in *AhRR(−/−)* mice, *Cyp1a1* mRNA continued to increase to a higher level than in WT mice throughout the course of the experiment. These results support the idea that AhRR represses AhR activity in WT mice.

In addition to spleen and stomach, 3MC treatment also induced the expression of *Cyp1a1* mRNA in the skin of *AhRR(−/−)* mice to a higher level than in WT skin (Fig. 2C).

Because both *AhR* [12] and *AhRR* disrupted genes were inserted in a reading frame of the respective genes with NLS-*LacZ*, we were able to examine the expression patterns of AhR and AhRR in the skin by β-galactosidase staining. AhRR expression was restricted to the dermal fibroblasts (Fig. 3A and C), while AhR was expressed in both fibroblasts and epidermal cells (Fig. 3B and D). To investigate the expression of AhRR and CYP1A1 in the dermal fibroblasts in detail, we isolated dermal fibroblasts from *AhRR(−/−)* and WT mice, and cultured them for treatment with B[*a*]P. *AhRR* mRNA was clearly induced in response to B[*a*]P in WT fibroblasts (Fig. 3E), whereas no expression of AhRR was observed in *AhRR(−/−)* cells. On the other hand, *AhRR(−/−)* fibroblast cells induced *Cyp1a1* mRNA in response to B[*a*]P to a level much higher

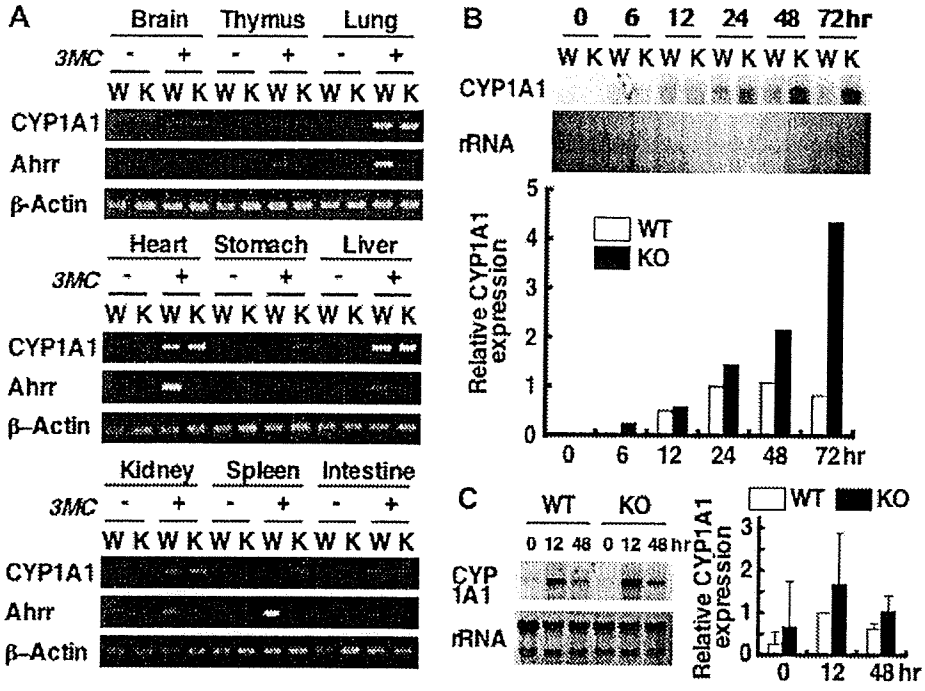

Fig. 2. Inducibility of *AhRR* and *Cyp1a1* mRNA in various tissues. (A) Expression of *Cyp1a1* and *AhRR* mRNA in various tissues of wild type (W) and *AhRR(−/−)* (K) mice. The mice were intraperitoneally injected with 3MC (80 mg/kg body weight). After 24 h, *Cyp1a1* and *AhRR* mRNA expression levels were examined by RT-PCR. Expression levels were normalized on the basis of β-actin expression. (B) A time course of *Cyp1a1* mRNA expression in spleen of wild-type (W) and *AhRR(−/−)* (K) mice after 3MC treatment. Wild-type or *AhRR(−/−)* mice were treated with 3MC; at indicated times after the treatment, RNA was extracted from spleen of the 3MC-treated mice and *Cyp1a1* mRNA expression was examined by RNA blot. *Cyp1a1* mRNA levels are presented relative to the wild-type value at 24 h. (C) Induction of *Cyp1a1* mRNA in skin of wild-type (WT) and *AhRR(−/−)* (KO) mice. 3MC was intraperitoneally injected into wild-type or *AhRR(−/−)* mice. RNA was extracted from the skin of the treated mice and used for determination of *Cyp1a1* mRNA by RNA blot. Average values of the four mice for each group are presented relative to the wild type at 12 h, with standard deviation.

than the wild type, and the induction continued to increase throughout the 24 h experiment. In contrast, wild-type cells slightly increased *Cyp1a1* mRNA but had decreased its expression by 24 h after the treatment. This "super-induction" of CYP1A1 in *AhRR(−/−)* skin fibroblast cells clearly suggest that AhRR works as a negative regulator of CYP1A1 in skin fibroblasts.

Skin carcinogenesis induced by B[a]P in AhRR KO mice

It is known that AhR mediates B[*a*]P carcinogenicity in the skin through expression of CYP1A1 [14]. We wished to investigate the carcinogenicity of B[*a*]P in the skin of *AhRR(−/−)* mice. Both *AhRR(−/−)* and WT mice were injected with B[*a*]P subcutaneously twice, a week apart, and the generation of skin carcinomas was observed thereafter (Fig. 4A). In WT mice, the first subcutaneous tumor was observed 12 weeks after the first treatment of B[*a*]P, and all the mice bore skin tumors 25 weeks after the treatment. On the other hand, the incidence of skin tumors in *AhRR(−/−)* mice was significantly delayed, ~5 weeks behind WT mice. Since CYP1A1 is known to be involved in both metabolic activation and detoxification of chemical carcinogens [16], these results suggest that overexpression of CYP1A1 shifts the balance of metabolic activity of *AhRR(−/−)* skin fibroblasts in favor of detoxification. Histological analysis of the tumors revealed that they were mostly fibrosarcomas, with a minor population of rhabdomyosarcomas and squamous cell carcinomas (data not shown), consistent with a previous report [14]. WT mice showed a slightly higher mortality than *AhRR(−/−)*, but without statistical significance (Fig. 4B).

Discussion

Previously, we reported that AhRR functions as a repressor of the AhR activity, based on transient DNA transfection experiments using cultured cell lines. AhRR represses the transactivation activity of AhR by competing with AhR for heterodimer formation with Arnt; the Arnt-AhRR heterodimer then competes for binding to XRE sequences [6]. To investigate the physiological roles of AhRR *in vivo*, we generated *AhRR(−/−)* mice by homologous gene recombination. The homozygous *AhRR(−/−)* mice were born at normal Mendelian ratios in genetic cross experiments using heterozygous AhRR mutant female and male mice. Mutants grew well and were fertile, indicating that AhRR is dispensable for mouse development and homeostasis. When given 3MC intraperitoneally as an inducer, *AhRR(−/−)* mice exhibited a higher level of CYP1A1 induction in the spleen, stomach and skin than WT mice. In contrast, CYP1A1 induction was not signifi-

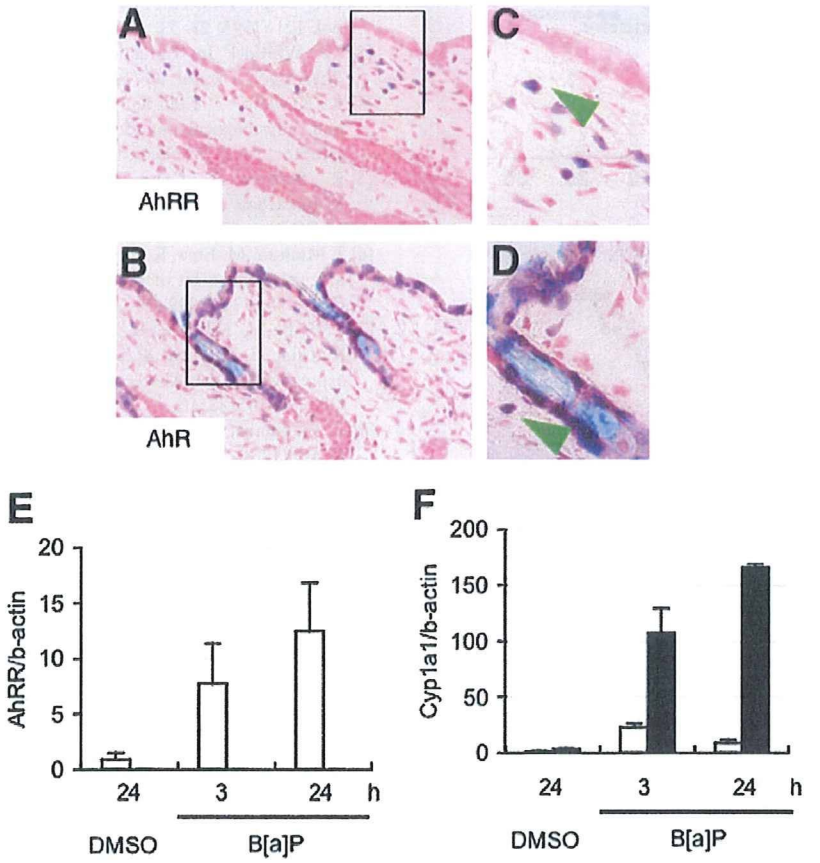

Fig. 3. Cyp1a1 and AhRR expressions in the skin and the skin fibroblast cells of wild-type and *AhRR(−/−)* mice. (A–D) AhRR and AhR expression in the skin. Skin sections prepared from *AhRR(−/−)* (A,C) or *AhR(+/−)* mice (B,D) were subjected to β-galactosidase staining for detection of AhRR or AhR expressing cells. Arrowheads indicate the blue (positive) signal in skin fibroblasts. (E) Expression of *AhRR* mRNA in the isolated skin fibroblast cells of wild-type mice after B[*a*]P treatment. Skin fibroblast cells were treated with vehicle (DMSO) or 1 mM B[*a*]P for 3 and 24 h. Total RNA was extracted from the treated cells and used for quantitation of AhRR by RT-PCR. (F) Expression of *Cyp1a1* mRNA in isolated skin fibroblast cells of wild-type and *AhRR(−/−)* mice after B[*a*]P treatment. Skin fibroblast cells were prepared from wild-type (open bars) and *AhRR(−/−)* mice (closed bars) as described above. The cultured cells were treated with B[*a*]P, and analyzed for *Cyp1a1* mRNA expression by the RT-PCR.

cantly affected in other tissues such as heart and lung, despite high inducibility of *AhRR* mRNA in these tissues of WT mice. Although the reason for this tissue-specific variation of the inducibility of CYP1A1 remains to be investigated, we speculate that protein levels of AhRR may vary from tissue to tissue, probably due either to stability of the protein or translational control. Recently, we have observed that the AhRR protein can undergo modifications, such as ubiquitination and sumoylation has been found to occur (our unpublished observations), and these alterations may be associated with the tissue-specific variation in the inducibility of *Cyp1a1* mRNA expression in *AhRR(−/−)* mice. Investigations of the detailed tissue-specific expression profiles of the AhRR protein are now underway. A study of expression of *LacZ*, which is knocked-in to the *AhR* and *AhRR* loci, revealed that AhR and AhRR are coexpressed in the skin fibroblasts under uninduced conditions. In the heterozygous *AhRR(+/−)* mice skin sections, we could not detect any ß-galactosidase staining, which was observed only in the skin of *AhRR(−/−)* mice (Fig. 3 and data not shown). This is probably because AhRR, which was expressed in *AhRR(+/−)* mice, repressed AhR activity; therefore, AhR-regulated *AhRR* expression was repressed below a detectable level in *AhRR(+/−)* mice. The lack of AhRR expression resulted in the enhancement of AhR activity, leading to the LacZ expression from the *LacZ*-knocked-in *AhRR* gene, in support of the notion that AhRR represses the AhR activity in the skin fibroblasts. These results are confirmed by the experiments using isolated skin fibroblast cells. *AhRR* mRNA was enhanced in WT cells in response to B[*a*]P, together with a slight, but significant enhanced expression of CYP1A1. On the other hand, induction of *Cyp1a1* mRNA was observed in *AhRR(−/−)* skin fibroblasts with significantly higher levels than WT.

AhR mediates carcinogenesis caused by chemical carcinogens through expression of CYP1A1 [14,17]. *AhRR(−/−)* mice are resistant to chemical carcinogenesis caused by B[*a*]P [14], because they have essentially no expression of CYP1A1. In this report, *AhRR(−/−)* mice were found to be relatively resistant to chemical carcinogenesis induced by B[*a*]P, as compared with WT mice. Since CYP1A1 is

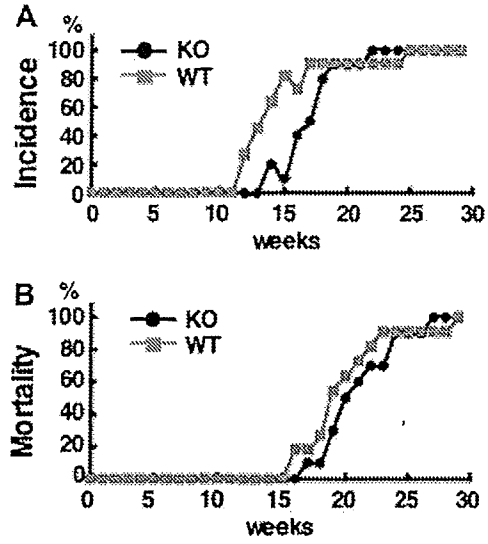

Fig. 4. B[*a*]P-induced tumor incidence and mortality of *AhRR(−/−)* mice. (A) WT (black; $n = 11$) and *AhRR*-KO (magenta; $n = 10$) mice were injected B[*a*]P subcutaneously twice. Tumor formation (A) and mortality (B) were observed as described in Materials and methods and shown as a percentage of the total.

known to be involved in both activation and detoxification of chemical carcinogens [16], "super-induction" of CYP1A1 in *AhRR(−/−)* mice is considered to shift the balance in favor of detoxification by accelerating the rate of drug metabolism to lower the carcinogenic intermediates of B[*a*]P.

Acknowledgments

We thank Yuko Kikuchi, Naomi Kaneko, Reiko Kawai, Mitsuru Okano and Masayoshi Noguchi for help during the experiments. We also thank Dr. Keisuke Yamashita and Ms. Yoko Nemoto for discussion and for clerical work, respectively. This work was supported in part by a grant from Solution Oriented Research for Science and Technology, Japan Science and Technology Agency and by a grant for Scientific Research from the Ministry of Health, Labor and Welfare of Japan.

References

[1] O. Hankinson, The aryl hydrocarbon receptor complex, Annu. Rev. Pharmacol. Toxicol. 35 (1995) 307–340.

[2] M.E. Hahn, The aryl hydrocarbon receptor: a comparative perspective, Comp. Biochem. Physiol. Part C Pharmacol. Toxicol. Endocrinol. 121 (1998) 23–53.

[3] J.P. Whitlock Jr., Induction of cytochrome P4501A1, Annu. Rev. Pharmacol. Toxicol. 39 (1999) 103–125.

[4] K. Kawajiri, Y. Fujii-Kuriyama, Cytochrome P450 gene regulation and physiological functions mediated by the aryl hydrocarbon receptor, Arch. Biochem. Biophys. 464 (2007) 207–212.

[5] R. Barouki, X. Coumoul, P.M. Fernandez-Salguero, The aryl hydrocarbon receptor, more than a xenobiotic-interacting protein, FEBS Lett. 581 (2007) 3608–3615.

[6] J. Mimura, M. Ema, K. Sogawa, Y. Fujii-Kuriyama, Identification of a novel mechanism of regulation of Ah (dioxin) receptor function, Genes Dev. 13 (1999) 20–25.

[7] T. Baba, J. Mimura, K. Gradin, A. Kuroiwa, T. Watanabe, Y. Matsuda, J. Inazawa, K. Sogawa, Y. Fujii-Kuriyama, Structure and expression of the Ah receptor repressor gene, J. Biol. Chem. 276 (2001) 33101–33110.

[8] T. Watanabe, I. Imoto, Y. Kosugi, Y. Fukuda, J. Mimura, Y. Fujii, K. Isaka, M. Takayama, A. Sato, J. Inazawa, Human arylhydrocarbon receptor repressor (AhRR) gene: genomic structure and analysis of polymorphism in endometriosis, J. Hum. Genet. 46 (2001) 342–346.

[9] H. Nishihashi, Y. Kanno, K. Tomuro, T. Nakahama, Y. Inouye, Primary structure and organ-specific expression of the rat aryl hydrocarbon receptor repressor gene, Biol. Pharm. Bull. 29 (2006) 640–647.

[10] S.I. Karchner, D.G. Franks, W.H. Powell, M.E. Hahn, Regulatory interactions among three members of the vertebrate aryl hydrocarbon receptor family: AHR repressor, AHR1, and AHR2, J. Biol. Chem. 277 (2002) 6949–6959.

[11] T. Hosoya, Y. Oda, S. Takahashi, M. Morita, S. Kawauchi, M. Ema, M. Yamamoto, Y. Fujii-Kuriyama, Defective development of secretory neurones in the hypothalamus of Arnt2-knockout mice, Genes Cells 6 (2001) 361–374.

[12] M. Ema, N. Ohe, M. Suzuki, J. Mimura, K. Sogawa, S. Ikawa, Y. Fujii-Kuriyama, Dioxin binding activities of polymorphic forms of mouse and human arylhydrocarbon receptors, J. Biol. Chem. 269 (1994) 27337–27343.

[13] E.C. Miller, J.A. Miller, Searches for ultimate chemical carcinogens and their reactions with cellular macromolecules, Cancer 47 (1981) 2327–2745.

[14] Y. Shimizu, Y. Nakatsuru, M. Ichinose, Y. Takahashi, H. Kume, J. Mimura, Y. Fujii-Kuriyama, T. Ishikawa, Benzo[a]pyrene carcinogenicity is lost in mice lacking the aryl hydrocarbon receptor, Proc. Natl. Acad. Sci. USA 97 (2000) 779–782.

[15] J. Mimura, K. Yamashita, K. Nakamura, M. Morita, T.N. Takagi, K. Nakao, M. Ema, K. Sogawa, M. Yasuda, M. Katsuki, Y. Fujii-Kuriyama, Loss of teratogenic response to 2,3,7,8-tetrachlorodibenzo-p-dioxin (TCDD) in mice lacking the Ah (dioxin) receptor, Genes Cells 2 (1997) 645–654.

[16] A. Conney, Induction of microsomal enzymes by foreign chemicals and carcinogenesis by polycyclic aromatic hydrocarbons: G.H.A. Clowes Memorial Lecture 42 (1982) 4875–4917.

[17] Q. Ma, Induction of CYP1A1. The AhR/DRE paradigm: transcription, receptor regulation, and expanding biological roles, Curr. Drug Metab. 2 (2001) 149–164.

Journal of Pharmacological and Toxicological Methods 58 (2008) 11–26

Contents lists available at ScienceDirect

Journal of Pharmacological and Toxicological Methods

journal homepage: www.elsevier.com/locate/jpharmtox

Original article

Interlaboratory validation of the modified murine local lymph node assay based on adenosine triphosphate measurement

Takashi Omori [a,*], Kenji Idehara [b,*], Hajime Kojima [c], Takashi Sozu [d], Kazunori Arima [e], Hirohiko Goto [f], Tomohiko Hanada [g], Yoshiaki Ikarashi [c], Taketo Inoda [h], Yukiko Kanazawa [i], Tadashi Kosaka [j], Eiji Maki [k], Takashi Morimoto [l], Shinsuke Shinoda [m], Naoki Shinoda [n], Masahiro Takeyoshi [o], Masashi Tanaka [p], Mamoru Uratani [q], Masahito Usami [r], Atsushi Yamanaka [s], Tomofumi Yoneda [t], Isao Yoshimura [u], Atsuko Yuasa [v]

[a] Kyoto University School of Public Health, Japan
[b] Daicel Chemical Industries Ltd., Japan
[c] National Institute of Health Sciences, Japan
[d] Osaka University, Japan
[e] Taisho Pharmaceutical Co. Ltd., Japan
[f] Otsuka Pharmaceutical Co. Ltd., Japan
[g] Nippon Shinyaku Co. Ltd., Japan
[h] Nakano Seiyaku Co. Ltd., Japan
[i] Food and Drug Safety Center, Japan
[j] Institute of Environmental Toxicology, Japan
[k] Biosafety Research Center, Foods, Drugs and Pesticides, Japan
[l] Sumitomo Chemical Co. Ltd., Japan
[m] Drug Safety Testing Center Co. Ltd., Japan
[n] Santen Pharmaceutical Co. Ltd., Japan
[o] Chemicals Evaluation and Research Institute, Japan
[p] Meiji Seika Kaisha Ltd., Japan
[q] Ishihara Sangyo Kaisha Ltd., Japan
[r] Hoyu Co. Ltd., Japan
[s] Pias Corporation, Japan
[t] Toa Eiyo Ltd., Japan
[u] Tokyo University of Science, Japan
[v] Fuji Film Co. Ltd., Japan

ARTICLE INFO

Article history:
Received 27 March 2008
Accepted 7 May 2008

Keywords:
Adenosine triphosphate
Interlaboratory validation
Local lymph node assay based on adenosine triphosphate content
Local lymph node assay
Skin sensitization
Methods

ABSTRACT

Introduction: The murine local lymph node assay (LLNA) is a well-established alternative to the guinea pig maximization test (GPMT) or Buehler test (BT) for the assessment of the skin sensitizing ability of drugs and chemicals. Daicel Chemical Industries Ltd. has developed a modified LLNA based on the adenosine triphosphate (ATP) content (LLNA-DA). We conducted 2 interlaboratory validation studies to evaluate the reliability and relevance of LLNA-DA. **Methods:** The experiment involved 17 laboratories, wherein 14 chemicals were examined under blinded conditions. In the first study, 3 chemicals were examined in 10 laboratories and the remaining 9 were examined in 3 laboratories. In the second study, 1 chemical was examined in 7 laboratories and the remaining 4 chemicals were examined in 4 laboratories. The data were expressed as the ATP content for each chemical-treated group, and the stimulation index (SI) for each chemical-treated group was determined as the increase in the ATP content relative to the concurrent vehicle control group. An SI of 3 was set as the cut-off value for exhibiting skin sensitization activity. **Results:** The results of the first study obtained in the experiments conducted for the 3 chemicals that were examined in all the 10 laboratories and for 5 of the remaining 9 chemicals were sufficiently consistent with small variations in their SI values. The sensitivity, specificity, and accuracy of LLNA-DA against those of GPMT/BT were 7/8 (87.5%), 3/3 (100%), and 10/11 (90.9%), respectively. In the second study, all the 5 chemicals studied demonstrated acceptably small interlaboratory variations. **Discussion:** In the first study, a large variation was observed for 2 chemicals; in the second study, this variation was small. It was attributed to the

* Corresponding authors. Omori is to be contacted at Department of Biostatistics, Kyoto University School of Public Health, Yoshida Konoe-cho, Sakyo-ku, Kyoto 606-8501, Japan. Tel.: +81 75 753 4482; fax: +81 75 753 4487. Idehara, Daicel Chemical Industries, Ltd., 1239 Shinzaike, Aboshi-ku, Himeji, Hyogo 671-1283, Japan. Tel.: +81 79 274 4096; fax: +81 79 274 5831.
E-mail addresses: omori@pbh.med.kyoto-u.ac.jp (T. Omori), kn_idehara@daicel.co.jp (K. Idehara).

1056-8719/$ – see front matter © 2008 Elsevier Inc. All rights reserved.
doi:10.1016/j.vascn.2008.05.001

application of dimethylsulfoxide as the solvent for the metallic salts. In conclusion, these 2 studies provide good evidence for the reliability of the LLNA-DA.

© 2008 Elsevier Inc. All rights reserved.

1. Introduction

Skin sensitization (allergic contact dermatitis (ACD)) is an immunologically mediated cutaneous reaction to a drug or chemical. It is known that detecting and evaluating the immune-based adverse effects that are collectively referred to as hypersensitivity reactions is a very difficult task, particularly during the drug approval process, because of the lack of adequate non-clinical models and the low incidence rate of reactions (Hastings, 2001). However, there are several adequate and predictive methods for modeling ACD. For several decades, tests involving guinea pigs, such as the guinea pig maximization test (GPMT) or the Buehler test (BT), have been used for assessing the skin sensitization potential of chemicals (OECD, 1992).

The local lymph node assay (LLNA) employs a mouse model for assessing the relative sensitization potential; it is a well-established alternative method for determining whether a chemical causes ACD. Although GPMT and BT can be viewed as phenomenological methods in which the clinical signs are modeled, LLNA was developed on the basis of a mechanistic understanding of immune-based contact dermatitis (Hastings, 2001). In addition, this method also offers important animal welfare benefits. The use of LLNA has been successfully validated by several studies (Basketter et al., 2002; Basketter, Gerberick, Kimber, & Loveless, 1996; Basketter & Scholes, 1992; Gerberick, Ryan, Kimber, Dearman, & Basketter, 2000; Haneke, Tice, Carson, Margolin, & Stokes, 2001). Recently, it has been recommended that this method be formally adopted by the Organization for Economic Co-operation and Development (OECD), according to the guidelines for testing chemicals 406 and 429 (OECD, 1992, 2002), and that it be accepted by the EU and US as a suitable method for classifying the skin sensitizing ability of chemicals (Basketter, Casati, Gerberick, Griem, Philips, & Worth, 2005; Dean, Twerdok, Tice, Sailstad, Hattan, & Stokes, 2001; Sailstad, Hattan, Hill, & Stokes, 2001). The LLNA was specifically designed to identify contact allergens. The assay was not intended to facilitate the detection of low molecular weight chemicals associated with systemic sensitization or drug allergies (Kimber, 2001). However, an investigation, which was designed to explore the ability of LLNA to identify pharmaceutical process intermediates known to cause contact allergy in humans, provided evidence that the assay is a useful method for hazard identification (Durand, De Burlet, Virat, & Nauman, 2003). Furthermore, presently, the use of the method, along with the use of GPMT and BT, is recommended for the determination of the skin sensitization potential of new drugs (FDA, 2002).

The original LLNA uses [^{3}H]-methyl thymidine to measure lymphocyte proliferation; this hinders it use, particularly in Japan, because being a radioisotope (RI)-based method, it requires special facilities. Several authors have been conducting investigations for the development of an alternative non-RI method for performing LLNA (Dearman, Hilton, Basketter, & Kimber,, 1999; Ehling et al., 2005a, 2005b; Hatao, Hariya, Katsumura, & Kato, 1995; Lee, Park, Park, Kim, & Oh, 2002; Takeyoshi, Yamasaki, Yakabe, Takatsuki, & Kimber, 2001).

Daicel Chemical Industries Ltd. proposed a modification of LLNA, which involves the measurement of the adenosine triphosphate (ATP) content instead of [^{3}H]-methyl thymidine incorporation for assessing lymphocyte proliferation (Idehara, Yamagishi, Yamashita, & Ito, in press; Yamashita, Idehara, Fukuda, Yamagishi, & Kawada, 2005). This modified assay method is designated as the LLNA modified by Daicel, based on the ATP content (LLNA-DA).

Although LLNA-DA essentially involves the same procedure as LLNA, the evidence available is insufficient for validating the assay method through interlaboratory evaluation. Therefore, we conducted 2 interlaboratory validation studies for LLNA-DA.

In the first study, 2 metallic salts—cobalt chloride and nickel sulfate—dissolved in dimethylsulfoxide (DMSO) produced inconsistent results across the laboratories. We assumed that the inconsistency factor would be due to one of the following 2 reasons: (1) DMSO was used as the vehicle in the control group for the 2 metallic salts, and DMSO application in mice is difficult as compared with acetone–olive oil (AOO) or acetone (ACE) application or (2) LLNA-DA is unsuitable for use with metallic salts, and both the chemicals used were metallic salts. Therefore, a second study employing additional metallic salt with DMSO was planned in order to ascertain the hypothesis.

The primary objectives of the first study were (1) to evaluate the extent of interlaboratory variation with regard to LLNA-DA and (2) to ascertain whether the results of LLNA-DA are comparable with those of LLNA. The primary objective of the second study was to examine the reliability of the LLNA-DA method when metallic salts were tested with DMSO.

2. Methods

2.1. Organization

This study was organized by researchers belonging to the committee for the validation of the assay. The research team comprised

Table 1(a)
Selected chemicals with their corresponding vehicles, the referenced results of LLNA and GPMT/BT, and the allocation of chemicals for the LLNA-DA experiments in the first study

Chemical	CASRN[a]	Vehicle[b]	LLNA	GPMT/BT[c]	Laboratory[d]									
					1	2	3	4	5	6	7	8	9	10
A: 2,4-Dinitrochlorobenzene	97-00-7	AOO	+	+	□	□	□	□	○	△	□	□	△	○
B: Hexyl cinnamic aldehyde	101-86-0	AOO	+	+	○	○	△	△	△	□	△	○	○	△
C: 3-Aminophenol	591-27-5	AOO	+	+nonstd	□		○					□		
D: Glutaraldehyde	111-30-8	ACE	+		△	△			□					
E: Cobalt chloride	7646-79-9	DMSO	+	+				○		○		△		
F: Isoeugenol	97-54-1	AOO	+	+				□	○				△	
G: Formaldehyde	50-00-0	ACE	+	+	△	△			□					
H: Dimethyl isophthalate	1469-93-4	AOO	−	−	□		□				□			
I: Isopropanol	67-63-0	AOO	−	−	○	○	△	△	△	□	△	○	○	△
J: Nickel sulfate	10101-97-0	DMSO	−	+				○		○		△		
K: Abietic acid	514-10-3	AOO	+	+		□				△	○			
L: Methyl salicylate	119-36-8	AOO	−	−			○				○			○

[a] The Chemical Abstract Services Registry Number.
[b] ACE, acetone; AOO, acetone–olive oil; DMSO, dimethylsulfoxide.
[c] Judgment based on the guinea pig maximization test or the Buehler test; "nonstd" indicates a nonstandard animal that was not tested for chemical C.
[d] Allocated pairs for the LLNA-DA experiments in a laboratory; ○, experiment 1; △, experiment 2; □, experiment 3.

Table 1(b)
Selected chemicals with their corresponding vehicles, the referenced results of LLNA and GPMT/BT, and the allocation of chemicals in the second study

Chemical	CASRN[a]	Vehicle[b]	LLNA	GPMT/BT[c]	Laboratory[d]						
					11	12	13	14	15	16	17
B: Hexyl cinnamic aldehyde	101-86-0	AOO	+	+	○	○	○	○	○	○	○
E: Cobalt chloride	7657-79-9	DMSO	+	+	□		△	△			△
J: Nickel sulfate	10101-97-0	DMSO	−	+	□	△		△		△	
M: Lactic acid	598-82-3	DMSO	−	−	△		△		△	△	
N: Potassium dichromate	7778-50-9	DMSO	+	+	△	△			△		△

[a] The Chemical Abstract Services Registry Number.
[b] ACE, acetone; AOO, acetone–olive oil; DMSO, dimethylsulfoxide.
[c] Judgment based on guinea pig maximization test or Buehler test.
[d] Allocated pairs for an experiment in a laboratory; ○, experiment 1; △, experiment 2; □, experiment 3.

representatives from each experimental laboratory, toxicologists as the chemical selectors and as distributors of the chemicals and materials, biostatisticians, and the study manager. All the experimentations were performed by the toxicologists of the experimental laboratories. In the first study, participation was limited to 10 experimental laboratories with sufficient experience in the use of the LLNA and/or its modifications; however, this was not a limiting factor in the second study, in which 7 additional experimental laboratories were included. A total of 17 different experimental laboratories participated in these 2 studies.

Research teams of all the experimental laboratories obtained ethical approval for each standard operational procedure conducted in their laboratories.

2.2. Technology transfer

A 1-day technology-transfer seminar was held by the LLNA-DA developer for each study, which was attended by at least 1 toxicologist from each experimental laboratory. Participants learned the method of conducting the assay according to the standard protocol. In addition, in the second study, the operation of LLNA-DA with DMSO was also included in the seminar (Omori et al., 2008).

2.3. Preliminary tests

Prior to each study, a preliminary test was conducted by researchers from all the experimental laboratories, who used only the positive control chemical, namely, 25% hexyl cinnamic aldehyde. The purpose of these preliminary tests was to ascertain whether the standard protocol was being documented sufficiently and to confirm the sensitivity of LLNA-DA (Omori et al., 2008).

The results of both preliminary tests revealed that the standard protocol was essentially valid and required few modifications.

2.4. Chemical selection and allocation

The chemical selectors chose 20 candidate chemicals that were previously used in LLNA and whose test results had been documented (Basketter & Scholes, 1992; Basketter, Gerberick, & Kimber, 1998; Basketter, Lea, Cooper, et al., 1999; Basketter, Lea, Dickens, 1999; Basketter, Blaikie, Dearman, Kimber, Ryan, Gerberick, et al., 2000; Gerberick et al., 2004; Haneke et al., 2001; Kimber et al., 1998; Loveless et al., 1996). On the basis of these literature data and solubility of the chemicals, the chemical selectors selected vehicles and prepared 3 fixed doses (low, medium, and high) for each chemical; subsequently, the chemicals were transported from the chemical and material distributors to the experimental laboratories.

In the first study, 12 of the 20 candidate chemicals were selected and classified as strong, mild, or weak sensitizers or non-sensitizers on the basis of LLNA. In order to reduce the number of animals used, pairs comprising groups treated with 2 or 3 chemicals and the same vehicle control group were employed; in other words, in each laboratory, 2 or 3 chemicals were simultaneously tested with 1 negative control and 1 positive control for every experiment. Of the 12 chemicals, 3 were dispatched to all the 10 participating experimental laboratories, and the remaining 9 were randomly allocated to the laboratories by a biostatistician and dispatched to each of the 3 experimental laboratories.

In the second study, 5 of the 20 candidate chemicals were selected. To determine whether the results from the 7 new laboratories would be similar to those obtained in the first study, the chemical selectors chose a single chemical that had been tested by all the 10 laboratories in the first study. The remaining 4 chemicals selected by the chemical selectors comprised 3 metallic salts—cobalt chloride, nickel sulfate, and potassium dichromate—and lactic acid with DMSO as the vehicle control. Pairs comprising groups treated with 2 of the 4 chemicals and

Table 2(a)
Body weight (g) [day 1]

Laboratory	n	Mean	SD	Min	Med	Max
1	120	22.0	1.5	19.3	21.8	27.1
2	108	22.5	1.3	19.4	22.6	25.0
3	108	22.0	1.2	18.2	22.0	24.8
4	108	22.7	1.4	20.0	22.5	26.7
5	108	21.6	1.1	19.1	21.6	24.4
6	108	21.7	1.4	19.3	21.7	24.9
7	108	22.8	1.4	18.5	22.8	25.9
8	108	23.4	1.5	20.5	23.3	28.6
9	72	23.0	1.2	20.1	22.9	26.5
10	72	22.6	1.4	19.8	22.5	25.8
11	96	22.9	1.3	19.9	22.9	26.5
12	60	21.6	1.0	18.8	21.7	24.1
13	60	22.2	1.1	19.5	22.1	24.8
14	60	21.8	1.5	18.7	21.8	24.3
15	60	22.5	1.1	20.0	22.5	25.2
16	60	22.3	1.5	18.8	22.6	25.5
17	60	22.1	1.4	19.5	22.3	26.4

Table 2(b)
Body weight (g) [day 8]

Laboratory	n	Mean	SD	Min	Med	Max
1	120	22.1	1.5	19.0	22.0	26.1
2	108	23.4	1.4	20.6	23.3	26.7
3	108	23.2	1.4	19.8	23.2	26.6
4	104	23.4	1.4	20.4	23.3	27.1
5	108	23.0	1.3	20.1	23.0	25.8
6	108	22.2	1.4	19.2	22.2	25.6
7	108	23.0	1.5	17.1	23.0	26.0
8	108	23.9	1.8	20.1	24.0	29.2
9	72	23.9	1.3	20.9	23.9	27.0
10	72	23.3	1.3	20.7	23.3	26.8
11	96	23.4	1.3	21.1	23.3	27.1
12	60	23.1	1.2	20.4	23.2	26.5
13	60	22.9	1.3	20.2	22.7	26.2
14	59	22.3	1.9	16.3	22.4	25.9
15	60	23.8	1.3	21.3	23.6	26.6
16	60	23.3	1.6	19.1	23.4	27.0
17	60	23.1	1.4	19.7	23.3	26.7

Table 3(a)
Mean and SD for the ATP content and SI values obtained in all the laboratories in the first study

Vehicle/ concentration	1		2		3		4		5		6		7		8		9		10	
	Mean±SD	SI	Mean±SD	SI	Mean±SD	SI	Mean±SD	SI	Mean±SD	SI	Mean±SD	SI	Mean±SD	SI	Mean±SD	SI	Mean±SD	SI	Mean±SD	SI
A: 2,4-Dinitrochlorobenzene																				
AOO	27,188±10,027	–	26,159±2157	–	35,610±7212	–	42,866±9956	–	11,899±7366	–	13,910±3921	–	22,466±3515	–	20,576±5546	–	26,842±9515	–	53,350±14,893	–
0.03%	77,305±25,181	2.8	60,843±19,746	2.3	80,548±34,265	2.3	127,990±23,651	3.0	18,107±3203	1.5	38,247±10,833	2.7	86,083±21,219	3.8	49,730±22,738	2.4	75,290±20,086	2.8	62,000±23,941	1.2
0.10%	147,161±32,102	5.4	70,451±26,337	2.7	150,579±23,446	4.2	210,206±57,119	4.9	45,691±21,305	3.8	59,302±19,598	4.3	121,021±23,461	5.4	62,571±30,199	3.0	112,282±36,388	4.2	112,163±22,420	2.1
0.30%	325,485±46,981	12.0	241,465±73,709	9.2	354,678±27,371	10.0	365,768±51,573	8.5	166,224±43,333	14.0	210,636±46,213	15.1	296,024±33,270	13.2	259,203±105,308	12.6	292,230±5423	10.9	251,172±40,569	4.7
B: Hexyl cinnamic aldehyde																				
AOO	24,583±5761	–	41,189±17,452	–	35,652±12,253	–	43,007±8931	–	19,146±6582	–	16,375±3953	–	29,925±6142	–	12,207±4127	–	29,602±8049	–	29,077±2876	–
5%	33,196±6535	1.4	56,291±5484	1.4	48,383±14,959	1.4	64,212±6709	1.5	23,417±6260	1.2	27,369±8594	1.7	46,148±14,005	1.5	16,616±4630	1.4	25,602±11,242	0.9	40,685±14,674	1.4
10%	73,884±14,255	3.0	109,204±15,298	2.7	82,040±12,032	2.3	138,873±51,932	3.2	35,432±14,357	1.9	38,327±9530	2.3	126,755±35,639	4.2	50,829±8197	4.2	65,640±27,871	2.2	79,321±10,548	2.7
25%	142,130±29,633	5.8	198,520±40,800	4.8	158,304±26,958	4.4	219,687±29,834	5.1	76,029±5733	4.0	90,067±27,828	5.5	212,285±50,835	7.1	124,803±34,287	10.2	114,791±13,669	3.9	101,984±21,546	3.5

C: 3-Aminophenol

Vehicle/concentration	1		3		8	
	Mean±SD	SI	Mean±SD	SI	Mean±SD	SI
AOO	27,188±10,027	–	24,047±3932	–	20,576±5546	–
1%	47,591±2668	1.8	33,875±4945	1.4	25,167±4299	1.2
3%	63,021±9400	2.3	42,352±11,487	1.8	40,921±10,896	2.0
10%	76,927±15,323	2.8	41,759±8243	1.7	49,037±8244	2.4

D: Glutaraldehyde

Vehicle/concentration	1		2		5	
	Mean±SD	SI	Mean±SD	SI	Mean±SD	SI
ACE	17,947±4929	–	38,044±13,217	–	16,439±6488	–
0.05%	25,594±9403	1.4	28,096±9168	0.7	17,024±5163	1.0
0.15%	72,748±20,584	4.1	48,980±8745	1.3	40,319±17,078	2.5
0.50%	89,767±21,798	5.0	129,110±31,985	3.4	42,237±6048	2.6

E: Cobalt chloride

Vehicle/concentration	4		6		8	
	Mean±SD	SI	Mean±SD	SI	Mean±SD	SI
DMSO	100,396±24,632	–	4184±2395	–	19,803±4451	–
0.30%	–±–	–	44,002±30,922	10.5	87,562±13,336	4.4
1.00%	203,895±24,479	2.0	44,465±23,293	10.6	131,004±34,534	6.6
3.00%	267,172±52,088	2.7	85,978±24,933	20.6	159,808±13,473	8.1

F: Isoeugenol

Vehicle/concentration	4		5		9	
	Mean±SD	SI	Mean±SD	SI	Mean±SD	SI
AOO	42,866±9956	–	11,899±7366	–	26,842±9515	–
1%	125,838±22,236	2.9	22,896±7449	1.9	69,256±20,292	2.6
3%	175,277±10,289	4.1	23,619±8830	2.0	86,598±20,489	3.2
10%	262,118±34,406	6.1	117,098±5209	9.8	190,392±38,486	7.1

G: Formaldehyde

Vehicle/concentration	1		2		5	
	Mean±SD	SI	Mean±SD	SI	Mean±SD	SI
ACE	17,947±4929	–	38,044±13,217	–	16,439±6488	–
0.5%	52,214±10,965	2.9	64,467±11,056	1.7	19,510±5239	1.2
1.5%	51,405±13,007	2.9	115,143±20,638	3.0	30,959±12,804	1.9
5.0%	86,934±33,582	4.8	120,966±21,688	3.2	44,219±7822	2.7

H: Dimethyl isophthalate

Vehicle/concentration	1		3		7	
	Mean±SD	SI	Mean±SD	SI	Mean±SD	SI
AOO	27,188±10,027	–	35,610±7212	–	22,466±3515	–
5%	36,534±10,199	1.3	35,710±8126	1.0	28,306±4047	1.3
10%	31,200±10,875	1.1	34,357±8364	1.0	25,555±3074	1.1
25%	30,030±10,456	1.1	23,900±3733	0.7	23,583±3751	1.0

I: Isopranol

Vehicle/concentration	1		2		3		4		5		6		7		8		9		10	
	Mean±SD	SI	Mean±SD	SI	Mean±SD	SI	Mean±SD	SI	Mean±SD	SI	Mean±SD	SI	Mean±SD	SI	Mean±SD	SI	Mean±SD	SI	Mean±SD	SI
AOO	24,583±5761	–	41,189±17,452	–	35,652±12,253	–	43,007±8931	–	19,146±6582	–	16,375±3953	–	29,925±6142	–	12,207±4127	–	29,602±8049	–	29,077±2876	–
10%	37,756±12,448	1.5	37,286±9163	0.9	36,155±7444	1.0	67,307±12,946	1.6	10,106±3170	0.5	32,233±26,281	2.0	43,446±17,986	1.5	14,797±2984	1.2	18,791±7645	0.6	26,480±4594	0.9
25%	27,101±2623	1.1	35,024±4878	0.9	23,465±7953	0.7	38,859±7172	0.9	14,531±1549	0.8	14,762±5342	0.9	27,285±10,469	0.9	12,387±3421	1.0	20,627±6175	0.7	30,676±5707	1.1
50%	28,723±3313	1.2	33,259±7651	0.8	30,822±4465	0.9	34,382±6421	0.8	13,581±3696	0.7	21,360±4957	1.3	24,776±3613	0.8	13,551±1001	1.1	15,039±3697	0.5	36,216±4960	1.2

J: Nickel sulfate

Vehicle/concentration	4		6		8	
	Mean±SD	SI	Mean±SD	SI	Mean±SD	SI
DMSO	100,396±24,632	–	4184±2395	–	19,803±4451	–
1%	116,266±22,468	1.2	21,990±7141	5.3	69,077±14,602	3.5
3%	153,074±35,051	1.5	27,966±6162	6.7	60,881±7880	3.1
10%	103,595±20,343	1.0	49,303±14,901	11.8	50,568±9846	2.6

K: Abietic acid

Vehicle/concentration	2		6		7	
	Mean±SD	SI	Mean±SD	SI	Mean±SD	SI
AOO	26,159±2157	–	13,910±3921	–	21,546±13,493	–
5%	55,039±8805	2.1	25,277±9139	1.8	40,328±8389	1.9
10%	91,706±17,069	3.5	57,615±12,621	4.1	85,827±24,030	4.0
25%	121,351±36,474	4.6	110,697±29,265	8.0	81,818±24,819	3.8

L: Methyl salicylate

Vehicle/concentration	3		7		10	
	Mean±SD	SI	Mean±SD	SI	Mean±SD	SI
AOO	24,047±3932	–	21,546±13,493	–	53,350±14,893	–
5%	25,764±7330	1.1	23,459±7751	1.1	33,663±5192	0.6
10%	26,361±6381	1.1	38,158±6803	1.8	41,698±7559	0.8
25%	37,359±10,622	1.6	29,881±11,569	1.4	44,426±13,600	0.8

(continued on next page)

Table 3(a) (continued)

Positive control (hexyl cinnamic aldehyde)

Vehicle/ concentration	1		2		3		4		5		6		7		8		9		10	
	Mean±SD	SI	Mean±SD	SI	Mean±SD	SI	Mean±SD	SI	Mean±SD	SI	Mean±SD	SI	Mean±SD	SI	Mean±SD	SI	Mean±SD	SI	Mean±SD	SI
AOO	23,639±5906	–	30,284±11,576	–	25,429±5894	–	44,371±9224	–	15,183±5554	–	10,447±4413	–	25,112±8035	–	18,428±4503	–	26,327±5484	–	22,309±6393	–
25%	147,032±30,059	6.2	153,995±35,670	5.1	144,091±18,550	5.7	243,877±42,495	5.5	72,877±19,820	4.8	84,748±16,459	8.1	136,327±26,932	5.4	101,382±22,894	5.5	140,388±23,895	5.3	113,209±18,835	5.1

ACE, acetone; AOO, acetone–olive oil; DMSO, dimethylsulfoxide.
Number of animals: 4 for all the tested chemicals, 8 for the positive controls of laboratories 9 and 10, and 12 for the positive controls of laboratories 1–8.

the same vehicle control group were employed. These 4 chemicals were randomly allocated by a biostatistician.

In order to avoid predicting the severity of the effects of each chemical, all the chemical names were coded into alphabetic characters, and they were labeled as low, medium, and high in terms of the concentration that enabled blinded distribution for both the studies. However, prior to the study, the researchers and toxicologists of the respective laboratories were informed of the identity of the 20 candidate chemicals and the corresponding control vehicles. This was done in order to ensure the safety of the chemists performing the experiments (e.g., with regard to proper disposal of the chemicals) and to prevent any anxiety that they would experience while handling unknown chemicals.

2.5. Development of LLNA-DA

The original LLNA measures the proliferation of draining lymph node cells (LNCs) via the incorporation of [^{3}H]-methyl thymidine into DNA and β scintillation counting. Although this approach to measure the activity of LNC is well established through many studies on the original LLNA, alternative approaches that do not require the use of radioisotopes are expected to be beneficial.

ATP is the main energy source for a majority of cellular functions, and it is an essential molecule for living cells. ATP activity is known to indicate the number of living cells. Therefore, measurement of the ATP content in the lymph node by a luciferin–luciferase assay is considered to be one of the surrogates of altered lymph node cellularity. The measurement of the ATP content of the lymph node involves determination of the cell number at the end of cell proliferation, while the measurement of [^{3}H]-methyl thymidine incorporation involves determination of the endpoint of cell proliferation. One of the benefits of measuring the ATP content is that it allows the use of commercially available reagent kits; in this method, the ATP content is expressed in terms of the chemiluminescence (relative light units, RLU) induced by the luciferin–luciferase reaction.

Yamashita, Idehara, Fukuda, Yamagishi, and Kawada (2005) used 3 chemicals to study the approach involving the measurement of the ATP content. They found that when the dosing schedule of the original LLNA was followed, the ATP measurement approach as well as the flow cytometric analysis of LNCs (Hatao, Hariya, Katsumura, & Kato, 1995) or the assessment of 5-bromo-2′-deoxyuridine (BrdU) incorporation into LNCs (Takeyoshi, Yamasaki, Yakabe, Takatsuki, & Kimber, 2001) tended to show lower stimulation indices (SIs) than the original LLNA. Hence, in order to increase lymph node proliferation, Yamashita et al. proposed pretreatment with 1% sodium lauryl sulfate (SLS) prior to the application of the test chemicals and an additional treatment with the tested chemical. Through their studies, these authors successfully increased the sensitivity of the ATP measurement approach, and the SI value of 3 obtained with this approach was considered to be comparable to that of the original LLNA. Additionally, these authors conducted 6 independent experiments using eugenol to determine the intralaboratory variation in the SI values of the ATP measurement approach. The mean and coefficient of variance of the SI values were 4.0% and 17.3%, respectively.

Daicel Chemical Industries Ltd. refined the ATP measurement approach, which was designated LLNA-DA. In addition to the original LLNA procedure, this ATP content measurement assay includes pretreatment with 1% SLS solution along with its application of the test chemicals on the seventh day; this strategy was expected to yield similar SI values, i.e., approximately 3, to those of the original LLNA. Therefore, this additional step enabled the use of the same cut-off point as that of the original LLNA. By the time the first validation study was conducted, Daicel Chemical Industries Ltd. had obtained some results for LLNA-DA by using the abovementioned cut-off point, in which the correlation coefficient of the EC3 value for LLNA and LLNA-DA for 10 chemicals was 0.90,

Table 3(b)
Mean and SD for the ATP content and SI values obtained in all the laboratories in the second study

B: Hexyl cinnamic aldehyde

Vehicle/concentration	11		12		13		14		15		16		17	
	Mean±SD	SI	Mean±SD	SI	Mean±SD	SI	Mean±SD	SI	Mean±SD	SI	Mean±SD	SI	Mean±SD	SI
AOO	21,328±8537	–	27,436±7629	–	24,739±6350	–	24,348±8236	–	31,189±10,511	–	28,421±8943	–	23,888±10,275	–
5%	32,306±7470	1.5	45,178±8970	1.6	35,059±13,111	1.4	50,408±15,075	2.1	46,853±7275	1.5	65,209±12,332	2.3	31,668±6045	1.3
10%	70,689±7059	3.3	94,494±20,913	3.4	110,638±34,223	4.5	88,935±49,202	3.7	78,471±11,510	2.5	146,720±30,935	5.2	110,331±13,800	4.6
25%	95,348±32,502	4.5	156,615±19,035	5.7	133,833±22,340	5.4	185,142±43,204	7.6	122,146±25,678	3.9	239,220±35,785	8.4	154,106±28,583	6.5

E: Cobalt chloride

Vehicle/concentration	11		13		14		17	
	Mean±SD	SI	Mean±SD	SI	Mean±SD	SI	Mean±SD	SI
DMSO	82,093±26,296	–	81,326±13,350	–	41,770±12,971	–	50,815±5671	–
1%	122,193±21,742	1.5	133,890±34,318	1.6	97,101±15,349	2.3	148,776±68,574	2.9
3%	141,919±33,024	1.7	199,335±5756	2.5	171,272±19,452	4.1	216,116±18,966	4.3
5%	165,350±10,204	2.0	206,394±16,349	2.5	177,705±46,577	4.3	256,978±54,531	5.1

J: Nickel sulfate

Vehicle/concentration	11		12		14		16	
	Mean±SD	SI	Mean±SD	SI	Mean±SD	SI	Mean±SD	SI
DMSO	82,093±26,296	–	83,046±6308	–	41,770±12,971	–	76,153±28,228	–
1%	53,652±8085	0.7	82,896±14,003	1.0	77,804±25,666	1.9	90,029±11,264	1.2
3%	65,034±25,414	0.8	103,345±24,614	1.2	65,200±11,620	1.6	118,932±13,811	1.6
10%	60,451±17,784	0.7	80,596±21,515	1.0	88,990±14,982	2.1	88,482±19,237	1.2

M: Lactic acid

Vehicle/concentration	11		13		15		16	
	Mean±SD	SI	Mean±SD	SI	Mean±SD	SI	Mean±SD	SI
DMSO	65,060±9211	–	81,326±13,350	–	49,353±21,291	–	76,153±28,228	–
5%	60,576±20,296	0.9	80,639±18,883	1.0	45,730±8622	0.9	69,247±15,579	0.9
10%	49,033±11,761	0.8	55,369±7627	0.7	47,928±15,171	1.0	60,621±11,273	0.8
25%	52,131±16,088	0.8	60,124±13,945	0.7	35,259±2939	0.7	69,108±14,746	0.9

N: Potassium dichromate

Vehicle/concentration	11		12		15		16	
	Mean±SD	SI	Mean±SD	SI	Mean±SD	SI	Mean±SD	SI
DMSO	65,060±9211	–	83,046±6308	–	49,353±21,291	–	50,815±5671	–
01%	123,936±17,967	19	157,464±29,682	19	131,244±35,222	27	165,248±46,056	33
0.3%	145,833±41,893	2.2	217,061±37,807	2.6	191,819±51,627	3.9	257,138±29,816	5.1
1.0%	311,009±24,188	4.8	338,610±33,485	4.1	296,431±75,377	6.0	323,834±60,878	6.4

Positive control (hexyl cinnamic aldehyde)

Vehicle/concentration	11		12		13		14		15		16		17	
	Mean±SD	SI	Mean±SD	SI	Mean±SD	SI	Mean±SD	SI	Mean±SD	SI	Mean±SD	SI	Mean±SD	SI
AOO	25,807±8795	–	30,147±6951	–	24,943±6509	–	27,245±7022	–	33,713±7937	–	37,383±5294	–	17,417.3±7195	–
25%	102,118±22,127	4.0	142,679±50,388	4.7	136,950±22,057	5.5	184,010±31,146	6.8	143,322±31,990	4.3	268,199±47,663	7.2	138,799±25,305	8.0

ACE, acetone; AOO, acetone–olive oil; DMSO, dimethylsulfoxide.
Number of animals: 4 for all the tested chemicals, 8 for the positive controls of laboratories 12–17, and 12 for the positive control of laboratory 11.

and the accuracy of LLNA-DA against LLNA for 18 chemicals was 89% (16/18) (in-house data).

The ATP content value is influenced by time, that is, it decreases over time. This is not emerge in the original LLNA since it involves the measurement of [^{3}H]-methyl thymidine incorporation. Daicel Chemical Industry Ltd. investigated it and found that the ATP content value is not influenced by a 10- to 20-min delay, while this value would be reduced to approximately 50% of its original value with a 2-h delay. Therefore, Daicel Chemical Industry Ltd. recommends that when LLNA-DA is conducted, all the procedural steps from lymph node excision to the determination of the ATP content be performed rapidly and without delay.

Very recently, Idehara et al. (in press) reported the details of the intralaboratory study on LLNA-DA.

2.6. Standard protocol of LLNA-DA for the studies

The standard protocol for the assay was prepared prior to the preliminary test and determined according to the time of commencement of the study. Three doses were prepared for each of the test chemicals.

The groups of female CBA/JNCrlj mice (n=4; Charles River Japan Inc., Kanagawa) were treated with the topical application of 25 μL of 1 of the 3 doses of the test chemicals or the vehicle control exclusively on the dorsum of both ears. Following pretreatment with 1% SLS for 1 h, daily treatments with the chemicals were performed for the first 3 days and, subsequently, on day 7. On day 8, the treated mice were sacrificed, and the draining auricular lymph nodes were excised. After recording the lymph node weight (LNW), the LNCs were ground

between 2 slide glasses and subsequently suspended in 1 mL of phosphate-buffered saline (PBS) with a cell scraper. The LNC suspension was mixed and diluted to 1% with PBS. The ATP content was determined using a commercially available kit (Kikkoman Co., Tokyo). ATP was extracted from 0.1 mL of the diluted LNC suspension for 20 s, following which 0.1 mL of a reagent containing luciferase was added and the bioluminescence (RLU) in 10 s was measured with a luminometer (Lumitester C-100; Kikkoman Co., Tokyo). A point to note is that after the death of the animal, the ATP content of the lymph node decreases over time. It is therefore desirable that the series of procedures from lymph node excision to the determination of the ATP content must be performed rapidly and without delay.

2.7. Database

A biostatistician created a database containing the LNW and ATP content data obtained for each mouse in all the experimental laboratories. For comparison, data from studies on the original LLNA were collected and included in the database.

2.8. Statistical methods

For each experimental group, the SI was defined as the increase in the ATP content in the chemical-treated group relative to that in the vehicle control group. An SI of 3 was defined as the cut-off value for the skin sensitization potential. In order to demonstrate the variability within the SI values, the confidence interval of the SI values was calculated (Omori & Sozu, 2007). A variance component, τ^2, estimated by a random effect model for the log-transformed SI, was used as a measure of the interlaboratory variations; this is similar to the meta-analysis technique used in clinical studies (Normand, 1999). Using the abovementioned random effect model, we estimated the weighted average as an overall estimate of the SI value recorded for each chemical dose. The EC3 is defined as the estimated concentration that yields an SI value of 3. The EC3 of the weighted average was estimated and classified into the appropriate chemical category (Gerberick et al., 2004). Finally, the sensitivity, specificity, accuracy, positive predictivity, and negative predictivity were calculated as measures of relevance on the basis of the weighted averages in order to assess the concordance of the LLNA-DA results with the LLNA or GPMT/BT results (OECD, 2005). These measures were not calculated in the second study because of a shortage of chemicals.

3. Results

3.1. Chemical selection

Tables 1(a) and 1(b) show the selected chemicals, the results of LLNA and GPMT/BT as references, and the results obtained for the chemicals allocated for the LLNA-DA experiments of both the studies.

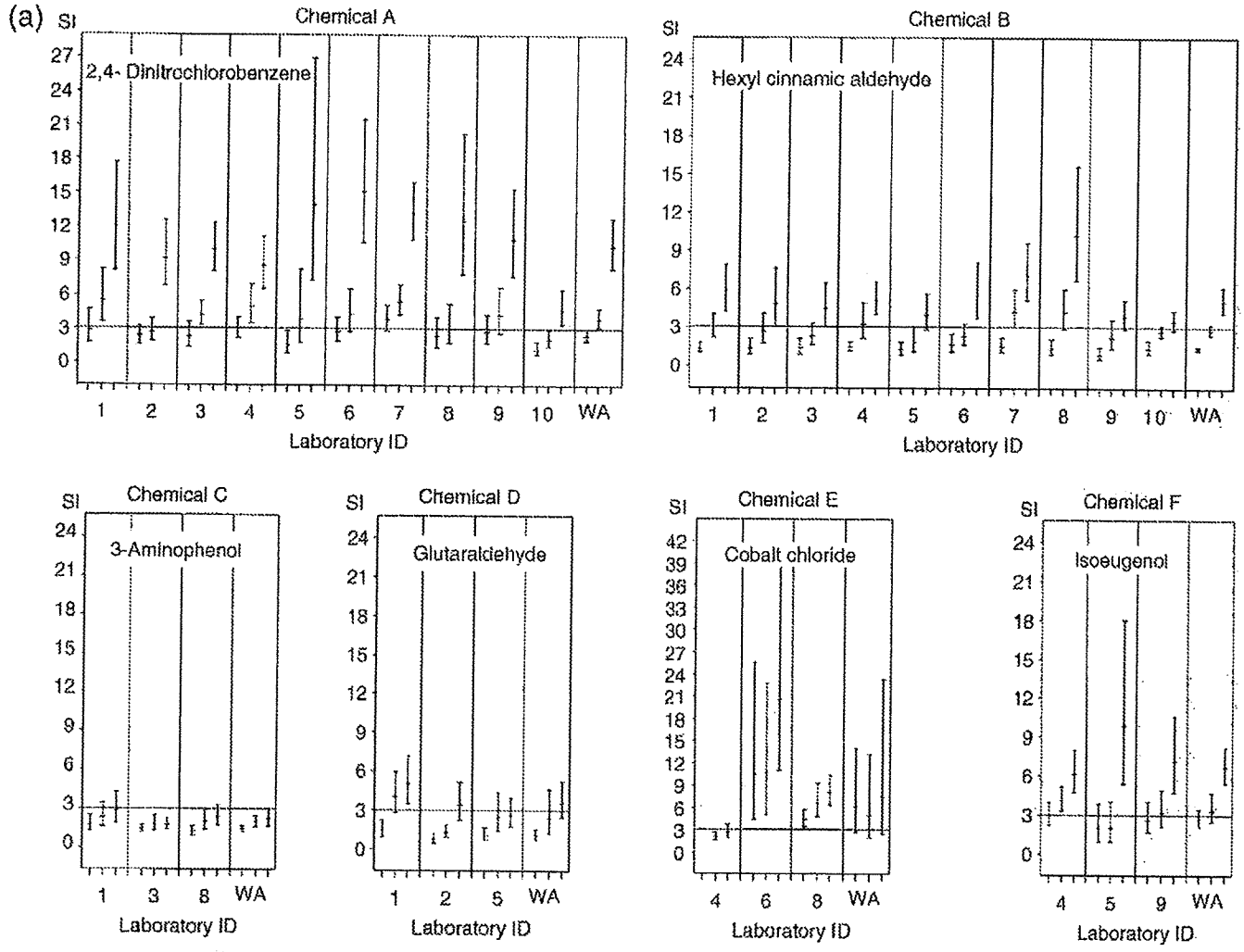

Fig. 1. (a). Dose–response relationships of the SI values with 95% confidence intervals for each chemical analyzed in all the laboratories. "WA" indicates the weighted average of the SI values obtained by meta-analysis using the random effect model in the first study. (b). Dose–response relationships of the SI values with 95% confidence intervals for each chemical analyzed in all the laboratories. "WA" indicates the weighted average of the SI values obtained by meta-analysis using the random effect model in the second study.